DECEMBER '25

INTERNATIONAL REVIEWS, RESEARCH AND STUDIES IN THE FIELD OF MATHEMATICS

EDITOR
PROF. DR. GÜNAY ÖZTÜRK

SERÜVEN YAYINEVİ

Genel Yayın Yönetmeni / Editor in Chief • C. Cansın Selin Temana

Kapak & İç Tasarım / Cover & Interior Design • Serüven Yayınevi

Birinci Basım / First Edition • © Aralık 2025

ISBN • 978-625-8671-20-9

Serüven Yayınevi / Serüven Publishing
Türkiye Adres / Turkey Address: Kızılay Mah. Fevzi Çakmak 1. Sokak
Ümit Apt No: 22/A Çankaya/ANKARA
Telefon / Phone: 05437675765
web: www.seruvenyayinevi.com
e-mail: seruvenyayinevi@gmail.com

Baskı & Cilt / Printing & Volume
Sertifika / Certificate No: 47083

INTERNATIONAL REVIEWS, RESEARCH AND STUDIES IN THE FIELD OF MATHEMATICS

EDITOR

PROF. DR. GÜNAY ÖZTÜRK

Contents

Chapter 1

IMPROVEMENTS ON FIBONACCI SEARCH METHOD IN OPTIMIZATION THEORY: A COMPREHENSIVE STUDY USING LUCAS AND K-LUCAS NUMBERS

Bünyamin Yıldız[1]

1 Department of Mathematics, Faculty of Arts and Sciences

Hatay Mustafa Kemal University, Hatay, Turkey

ORCID-ID: 0000-0002-0792-9520

1. Introduction

Optimization theory is central to addressing problems that arise in engineering, economics, physics, and many other scientific fields. Traditional optimization approaches are mainly designed to identify optimal points of functions that are continuous and differentiable. These approaches are analytical in nature and rely heavily on tools from differential calculus to determine optimality conditions. However, many real-world problems involve objective functions that lack continuity or differentiability, which limits the applicability of classical optimization methods in practice.

Calculus-based optimization techniques are applicable to functions that are continuous and at least twice differentiable. In this framework, evaluating the numerical value of the objective function typically comes at the final stage of the analysis, after the optimal values of the decision variables have been determined analytically. Despite these limitations, studying calculus-based methods is essential, as they provide the theoretical foundation for the development of most numerical optimization techniques.

In contrast, numerical optimization methods—such as the Fibonacci search method—follow a fundamentally different strategy. Instead of deriving optimality conditions analytically, these methods begin by computing the objective function at various candidate points and then use these evaluations to infer the location of the optimum. This feature makes numerical methods particularly advantageous, as they can be applied to objective functions that are non-differentiable or even discontinuous, thereby offering greater flexibility for practical applications.

Among the elimination methods, the Fibonacci search method is regarded as the best one to find the optimal point for single-valued functions. It is the most efficient derivative-free method for minimizing strict unimodal functions over a closed bounded interval, requiring the smallest number of iterations for a given reduction in the length of the interval of uncertainty. This chapter presents improvements on the classical Fibonacci search algorithm by employing Lucas numbers and k-Lucas numbers instead of conventional Fibonacci numbers, achieving faster convergence and more accurate results.

2. Theoretical Background

2.1. Fibonacci Numbers and the Golden Ratio

The Fibonacci sequence, named after the Italian mathematician Leonardo of Pisa (c. 1170–1250), also known as Fibonacci, is one of the most famous integer sequences in mathematics. It appears extensively in natural phenomena, from the arrangement of leaves on a stem to the spiral patterns in shells and sunflowers. The sequence is formally defined as follows:

$F_0 = 0, F_1 = 1,$ *and for* $n > 1$: $F_n = F_{n-1} + F_{n-2}$

The first terms of the Fibonacci sequence are: 0, 1, 1, 2, 3, 5, 8, 13, 21, 34, 55, 89, 144, 233, 377, ... One of the most remarkable properties of Fibonacci numbers is their relationship to the golden ratio φ (phi). As n increases, the ratio of consecutive Fibonacci numbers converges to the golden ratio:

$\lim (n\to\infty)\ F_{n+1}/F_n = \varphi = (1 + \sqrt{5})/2 \approx 1.6180339887...$

The golden ratio possesses unique mathematical properties that make it invaluable in optimization. It satisfies the equation $\varphi^2 = \varphi + 1$, and its reciprocal equals $\varphi - 1$. These properties ensure optimal interval reduction in search algorithms, as the golden ratio provides the most efficient way to divide an interval while maintaining the ability to reuse previous function evaluations.

2.2. Lucas Numbers and Their Properties

Lucas numbers, named after the French mathematician François Édouard Anatole Lucas (1842–1891), form a sequence closely related to Fibonacci numbers. Lucas made significant contributions to number theory and is perhaps best known for proving the primality of the Mersenne number $2^{127} - 1$. The Lucas sequence is defined with different initial conditions:

$L_0 = 2, L_1 = 1,$ *and for* $n > 1$: $L_n = L_{n-1} + L_{n-2}$

The first terms of the Lucas sequence are: 2, 1, 3, 4, 7, 11, 18, 29, 47, 76, 123, 199, 322, ... Like Fibonacci numbers, the ratio of consecutive Lucas numbers also converges to the golden ratio. Several important relationships exist between Fibonacci and Lucas numbers:

$L_n = F_{n-1} + F_{n+1}$

$L_n^2 - 5F_n^2 = 4(-1)^n$

$F_n + L_n = 2F_{n+1}$

These relationships demonstrate that Lucas numbers provide an alternative basis for optimization algorithms, with potentially different convergence characteristics compared to Fibonacci numbers.

2.3. Generalized k-Fibonacci and k-Lucas Numbers

The concept of Fibonacci numbers can be generalized to higher orders, leading to the k-Fibonacci sequence. For a positive integer $k \geq 2$, the k-Fibonacci sequence $\{g_n^{(k)}\}$ is defined as:

$g_1^{(k)} = g_2^{(k)} = \ldots = g_{k-2}^{(k)} = 0, g_{k-1}^{(k)} = g_k^{(k)} = 1$

and for $n > k$:

$g_n^{(k)} = g_{n-1}^{(k)} + g_{n-2}^{(k)} + \ldots + g_{n-k}^{(k)}$

The k-Lucas sequence is subsequently defined using k-Fibonacci numbers:

$l_n^{(k)} = g_{n-1}^{(k)} + g_{n+k+1}^{(k)}$ *for* $n \geq 1$

The initial values are given by $l_j^{(k)} = 2^{j-1}$ for $j = 1, 2, \ldots, k-1$, and $l_k^{(k)} = 2^{k-1} + 1$. For example, with $k = 5$, the 5-Lucas sequence begins: 1, 2, 4, 8, 17, 32, 63, 124, 244, 480, 943, 1854, 3645, 7166, ... These generalized sequences provide additional flexibility in designing optimization algorithms with varying convergence properties.

2.4. Unimodal Functions and Optimization Principles

A unimodal function is one that has only one peak (maximum or minimum) in a given interval. Formally, a function of one variable f(x) is said to be unimodal on an interval [a, b] if, given that two values of the variable are on the same side of the optimum, then the one nearer the optimum gives the better functional value—that is, the smaller value in the case of a minimization problem.

Importantly, a unimodal function can be non-differentiable or even discontinuous. If a function is known to be unimodal in a given range, the interval in which the minimum lies can be narrowed down provided the function values are known at two different points in the range. The assumption of unimodality is made in all elimination techniques, including Fibonacci search. If a function is known to be multimodal, the range must be subdivided into several parts, with each part treated separately as a unimodal function.

The theoretical advantage of zero-order methods, like the Fibonacci and golden section search, lies in their ability to operate without requiring differentiability of the unimodal function. This makes

them widely applicable to real-world problems where objective functions may not have well-defined derivatives.

3. Classical Fibonacci Search Method

The Fibonacci search method, originally developed by Kiefer (1953), is a technique for finding the maximum or minimum of a unimodal function. To apply the Fibonacci search method in a practical problem, the following criteria must be satisfied:

(i) The initial interval of uncertainty, in which the optimum lies, must be known.
(ii) The function being optimized must be unimodal in the initial interval of uncertainty.
(iii) The exact optimum cannot be located by this method. Only an interval, known as the final interval of uncertainty, will be known. The final interval of uncertainty can be made as small as desired by making more computations.
(iv) The number of function evaluations to be used in the search or the resolution required must be specified beforehand.

3.1. Algorithm Description

Consider the minimization problem where we seek to find the minimum of a unimodal function f(x) on the interval [a, b]. Let F_n denote the nth Fibonacci number, and let n be the predetermined number of iterations. The classical Fibonacci search algorithm proceeds as follows:

Step 1. Initialize the interval $[a_1, b_1] = [a, b]$ and set the iteration counter $k = 1$.
Step 2. Calculate the two interior points:

$$x_k = a_k + (b_k - a_k) \times F_{n-k+1}/F_{n-k+3}$$

$$x'_k = a_k + (b_k - a_k) \times F_{n-k+2}/F_{n-k+3}$$

Step 3. Evaluate the function values $f(x_k)$ and $f(x'_k)$.
Step 4. Update the interval: If $f(x_k) \leq f(x'_k)$, then $[a_{k+1}, b_{k+1}] = [a_k, x'_k]$. Otherwise, $[a_{k+1}, b_{k+1}] = [x_k, b_k]$.
Step 5. If $k + 1 \neq n$, increment k and go to Step 2. Otherwise, terminate the iteration.

The key property of this algorithm is that the points x_k and x'_k are symmetric with respect to the midpoint of the interval $[a_k, b_k]$. In each iteration, exactly one new function evaluation is required (the other point coincides with a point from the previous iteration), making the method highly efficient.

4. Improved Fibonacci Search Method with Lucas Numbers

The improvement on Fibonacci search method using Lucas numbers was proposed by Subasi, Yildirim, and Yildiz (2004). This approach replaces the Fibonacci numbers with Lucas numbers in the calculation of interior points, leading to partial improvements in locating intervals containing optimal points.

4.1. Algorithm with Lucas Numbers

Let L_k denote the kth Lucas number. The improved algorithm for minimizing a unimodal function f(x) on the interval [a, b] proceeds as follows:

Step 6. Initialize a, b, f(x), and set n (number of iterations).
Step 7. Set $[a_1, b_1] = [a, b]$ and $k = 1$.
Step 8. Calculate the interior points:

$$x_k = a_k + (b_k - a_k) \times L_{n-k+1}/L_{n-k+3}$$

$$x'_k = a_k + (b_k - a_k) \times L_{n-k+2}/L_{n-k+3}$$

Step 9. Calculate the values $f(x_k)$ and $f(x'_k)$.
Step 10. If $f(x_k) \leq f(x'_k)$, then $[a_{k+1}, b_{k+1}] = [a_k, x'_k]$. Otherwise, $[a_{k+1}, b_{k+1}] = [x_k, b_k]$.
Step 11. If $k + 1 \neq n$, increment k and go to Step 3. Otherwise, stop the iteration.

4.2. Error Estimation and Convergence Analysis

In each iteration (for $2 \leq k \leq n$), the length of the interval is given by:

$$b_k - a_k = (b - a) \times L_{n-k+3}/L_{n+2}$$

The optimal point estimate $\hat{x}$ is calculated as the midpoint of the final interval:

$$\hat{x} = a_n + (b_n - a_n)/2$$

The error of the improved method is bounded by:

$$|\hat{x} - x^*| \leq \tfrac{1}{2}(b_n - a_n) = (b - a) \times 1/L_{n+2}$$

The use of Lucas numbers results in different interval reduction ratios compared to Fibonacci numbers, which can lead to faster convergence in certain cases, particularly for smaller numbers of iterations.

5. Generalized Fibonacci Search Method with k-Lucas Numbers

A further generalization was proposed by Yildiz and Karaduman (2003), who employed k-Lucas numbers instead of conventional Fibonacci numbers and Lucas numbers. This approach provides even more improvements on the location of intervals containing optimal points in the classical Fibonacci search algorithm.

5.1. Algorithm with k-Lucas Numbers

Let $l_m^{(k)}$ denote the mth k-Lucas number. The generalized algorithm proceeds as follows:

Step 12. Initialize a, b, f(x), and set n (number of iterations) and k (order of Lucas numbers).
Step 13. Set $[a_1, b_1] = [a, b]$ and $m = 1$.
Step 14. Calculate the interior points:

$$x_m = a_m + (b_m - a_m) \times l_{n-m+1}^{(k)}/l_{n-m+3}^{(k)}$$

$$x'_m = a_m + (b_m - a_m) \times l_{n-m+2}^{(k)}/l_{n-m+3}^{(k)}$$

Step 15. Calculate $f(x_m)$ and $f(x'_m)$.
Step 16. If $f(x_m) \leq f(x'_m)$, then $[a_{m+1}, b_{m+1}] = [a_m, x'_m]$. Otherwise, $[a_{m+1}, b_{m+1}] = [x_m, b_m]$.
Step 17. If $m + 1 \neq n$, increment m and go to Step 3. Otherwise, stop.

5.2. Interval Length and Error Bound

In each iteration (for $2 \leq m \leq n$), the interval length is:

$$b_m - a_m = (b - a) \times l_{n-m+3}^{(k)}/l_{n+2}^{(k)}$$

The error bound for the generalized method is:

$$|\hat{x} - x^*| \leq (b - a) \times 1/l_{n+2}^{(k)}$$

The choice of k affects the convergence properties of the algorithm. Different values of k produce different interval reduction patterns, allowing optimization practitioners to select the most appropriate variant for their specific problem.

6. Numerical Results and Comparisons

To compare the classical Fibonacci search method with the improved methods, extensive numerical experiments were conducted using well-known test functions from optimization theory. Computer programs were developed in MAPLE to implement and compare these algorithms.

6.1. Test Function 1: Non-smooth Optimization Problem

The first test function, proposed by Ratz (1999) for nonsmooth global optimization, is:

$f(x) = |((x-1)/4)| + |sin(\pi(1 + (x-1)/4))| + 1$

This function is evaluated on the interval [-3, 3]. The true minimum point is x* = 1.0, with minimum value f(x*) = 1.0000. This function presents challenges for optimization algorithms due to its non-smooth nature.

Table 1. Comparison of classical and Lucas-improved methods for Test Function 1

n	Classical Interval	Improved Interval	Classical f*	Improved f*
2	[-1.00, 3.00]	[-0.4286, 3.00]	2.50000	1.29394
4	[0.00, 1.50]	[0.333, 1.667]	1.50768	1.00000
10	[0.958, 1.042]	[0.969, 1.043]	1.04313	1.00643
20	[0.9995, 1.0005]	[0.9997, 1.0003]	1.00023	1.00000
30	[0.99999, 1.00000]	[0.99999, 1.00000]	1.00000	1.00000

Table 2. Results with 3-Lucas numbers for Test Function 1 (k = 3)

k = 3	Classical	k-Lucas Improved	Classical f*	Improved f*
n = 4	[0, 1.500]	[0.143, 1.929]	1.50768	1.03697
n = 8	[0.927, 1.455]	[0.821, 1.093]	1.07527	1.04436
n = 16	[0.998, 1.003]	[0.996, 1.003]	1.00160	1.00051

6.2. Test Function 2: Multi-modal Appearance Problem

The second test function, from Törn and Žilinskas (1989), is more challenging:

$f(x) = \Sigma_{i=1}^{10} 1/[(k_i(x - a_i))^2 + c_i]$

where the parameters a, k, and c are vectors with 10 components each. This function is evaluated on the interval [-4, 5.2], with the true minimum at x* = -4.855 and f(x*) = -13.92234. The results demonstrate that the improved methods consistently outperform the classical Fibonacci search, particularly for lower iteration counts.

Table 3. Results for Test Function 2 with various k-Lucas numbers

Method	n = 5	n = 10	n = 15	True Value
Classical	-13.7369	-13.9195	-13.9224	-13.9223
Lucas	-13.8686	-13.9221	-13.9223	
4-Lucas	-13.8509	-13.9220	-13.9223	
5-Lucas	-13.8195	-13.9217	-13.9223	

6.3. Analysis of Results

The numerical results demonstrate several important findings. First, the improved methods using Lucas and k-Lucas numbers consistently produce smaller final intervals compared to the classical Fibonacci search method for the same number of iterations. Second, the optimal values of the objective functions are more accurate in the improved methods, particularly for smaller iteration numbers. Third, the advantage of the improved methods is most pronounced for $n < 20$, while for larger iteration counts, all methods converge to similar results.

The choice of k in the k-Lucas approach affects performance differently depending on the problem. For the test functions considered, $k = 3$ and $k = 4$ generally provided the best results, but the optimal choice may vary for different problem characteristics.

7. Recent Developments and Applications

The improvements on Fibonacci search methods using Lucas and k-Lucas numbers have inspired numerous subsequent studies and practical applications over the past two decades.

7.1. Parametrized Fibonacci Search Methods

Demir, Ömür, and Ulutaş (2008) presented a mathematical analysis of the Fibonacci search method by k-Lucas numbers, developing a new algorithm that determines the maximum point of unimodal functions on closed intervals. Their work demonstrated that this approach makes the Fibonacci search method more effective for finding maxima.

Subsequently, Ömür, Demir, and Ulutaş (2008) introduced a parametrized Fibonacci search method with k-Lucas numbers by introducing a parameter α that depends on the length of the interval and the function. This parameter ensures that the result obtained at the end of computation is correct. The parametrized approach provides additional flexibility in algorithm design, allowing practitioners to tune the method for specific problem characteristics.

7.2. Generalized Fibonacci Search Methods

Chong, Leow, and Sim (2021) developed a generalized Fibonacci search method for one-dimensional unconstrained non-linear optimization of unimodal functions. Their method uses the idea of "ratio length of 1" from the golden section search. The method takes successive lower Fibonacci numbers as the initial ratio and does not specify beforehand the number of iterations to be used. Evaluations using nine one-dimensional benchmark functions demonstrated that the generalized Fibonacci search method outperformed the golden section and other Fibonacci-type search methods, including Fibonacci, Lucas, and Pell approaches.

Rahman and Shaikh (2023) extended the Fibonacci search technique to interval optimization problems, developing c-r and c-L Fibonacci search methods based on interval order relations. This extension allows the handling of imprecise objective functions, which is particularly relevant for real-world applications where exact function values may not be available.

7.3. Practical Applications

The improved Fibonacci search methods have found applications in diverse fields:

Inventory Optimization: Simulation-driven Lucas search has emerged as a powerful tool for optimizing complex inventory management systems, particularly in the context of (Q, r) inventory policies where Q represents the order quantity and r denotes the reorder point. The methodology employs a sophisticated "one at a time" approach, systematically applying Lucas search to each decision variable while holding others constant. This sequential optimization strategy creates a convergent sequence of parameter values that progressively refine the inventory policy.

The advantages of this approach are particularly pronounced in stochastic inventory environments where demand uncertainty and lead time variability create complex, nonlinear objective functions. Traditional gradient-based methods often struggle with the discontinuities and noise inherent in simulation-based inventory models, whereas the Lucas search methodology maintains robustness through its derivative-free nature. The method has been successfully implemented in multi-echelon supply chain systems, where it efficiently navigates the high-dimensional parameter space to identify near-optimal policies. Furthermore, the computational efficiency of Lucas search—requiring fewer function evaluations than exhaustive grid search or genetic algorithms—makes it particularly suitable for real-time inventory optimization in dynamic business environments where rapid decision-making is critical.

Textile Thermal Conductivity Determination

The parametrized Fibonacci search method has proven invaluable in solving inverse problems within textile engineering, specifically addressing the challenging task of determining thermal conductivity coefficients from experimental temperature and moisture data. This application is particularly critical in the design of protective clothing for extreme cold environments, where accurate thermal property characterization directly impacts wearer safety and comfort.

The inverse problem formulation involves matching predicted temperature distributions from nonlinear heat and moisture transfer models to experimentally measured values, with thermal conductivity as the unknown parameter to be estimated. The nonlinearity arises from the coupled nature of heat and moisture transport, where moisture migration affects thermal properties, which in turn influences moisture diffusion. Traditional inverse methods such as least-squares estimation or Newton-Raphson iteration often encounter convergence difficulties due to the ill-posed nature of these problems and the presence of multiple local minima.

The parametrized Fibonacci search addresses these challenges through systematic interval reduction guided by Fibonacci ratios, ensuring convergence to physically meaningful thermal conductivity values. The parametrization aspect allows incorporation of prior knowledge about feasible thermal conductivity ranges for different textile materials, effectively constraining the search space and improving solution uniqueness. This method has been validated against experimental data from textile samples subjected to temperatures as low as -40°C, demonstrating accuracy within 3-5% of reference values obtained through direct measurement techniques. The robustness of this approach has facilitated its adoption in quality control processes for technical textile manufacturing and in the development of advanced thermal insulation materials.

Adaptive Beamforming

A novel Fibonacci branch search (FBS) optimizer represents a significant advancement in adaptive beamformer design for antenna arrays and signal processing applications. The method leverages hierarchical tree branch structures combined with interactive searching rules fundamentally inspired by the golden ratio properties inherent in the Fibonacci sequence. This approach addresses the critical challenge of simultaneously achieving low sidelobe levels and deep null placement in the radiation pattern, which is essential for interference rejection and signal-to-interference-plus-noise ratio (SINR) maximization.

The FBS optimizer operates by constructing a decision tree where each branch corresponds to a potential weight coefficient adjustment for the antenna array elements. The branching strategy follows Fibonacci sequence principles, allocating search effort proportionally to regions of the weight space that show promise for improved beamforming performance. This creates an adaptive search density that concentrates computational resources in high-potential areas while maintaining global exploration capabilities.

Comparative studies have demonstrated that FBS achieves sidelobe levels 8-12 dB lower than conventional minimum variance distortionless response (MVDR) beamformers while placing nulls with depths exceeding 40 dB in interference directions. The method exhibits particular strength in

scenarios with multiple coherent interferers, where traditional adaptive algorithms often experience performance degradation. Additionally, the FBS optimizer shows excellent convergence characteristics, typically requiring 40-60% fewer iterations than particle swarm optimization or genetic algorithm implementations for equivalent beamforming performance. These attributes have led to its implementation in advanced radar systems, satellite communication terminals, and 5G/6G wireless base stations where precise spatial filtering is paramount.

Structural Health Monitoring

Tran-Ngoc and colleagues (2023) introduced a groundbreaking approach that synthesizes Fibonacci sequence-based optimization with the Salp Swarm Algorithm (SSA) for large-scale railway bridge monitoring systems. This hybrid methodology, termed Golden Salp Swarm Algorithm (GSSA), addresses the computational challenges inherent in continuous structural health monitoring of extensive railway infrastructure networks.

Railway bridges present unique monitoring challenges due to their exposure to repetitive dynamic loading from train passages, environmental factors such as temperature fluctuations and corrosion, and the critical safety implications of structural deterioration. Traditional monitoring approaches based on dense sensor arrays and finite element model updating become computationally prohibitive for bridge networks spanning hundreds of kilometers. The GSSA approach tackles this scalability challenge through intelligent search space exploration guided by golden ratio principles.

The algorithm employs the Fibonacci golden ratio to modulate the exploration-exploitation balance in the salp swarm's chain formation behavior. Specifically, the leader salp's position update incorporates golden ratio weighting factors that determine the relative influence of the food source (optimal solution) versus random exploration. This modification enhances the algorithm's ability to escape local optima—a common problem in structural damage identification where multiple damage scenarios may produce similar sensor response patterns.

Field validation studies on operational railway bridges have demonstrated that GSSA reduces computational time by 55-70% compared to conventional genetic algorithms while improving damage localization accuracy by 15-25%. The method successfully identifies multiple simultaneous damage locations, quantifies damage severity levels, and operates reliably even with incomplete sensor data—a common practical constraint in real-world monitoring systems. This approach has been integrated into several national railway infrastructure monitoring programs, providing continuous assessment of bridge health conditions and enabling proactive maintenance scheduling.

Feature Selection in Machine Learning

The Golden Lichtenberg Algorithm (GLA), introduced in 2024, represents a sophisticated fusion of Fibonacci sequence principles with Lichtenberg figure-inspired search patterns for high-dimensional feature selection problems. Feature selection is crucial in machine learning applications where datasets contain hundreds or thousands of potential predictive variables, many of which may be irrelevant or redundant. Selecting optimal feature subsets improves model interpretability, reduces overfitting, and decreases computational requirements for training and inference.

The GLA draws inspiration from the fractal branching patterns of Lichtenberg figures (the tree-like patterns formed by electrical discharges) combined with golden ratio-based step size adaptation. The algorithm maintains a population of candidate feature subsets that explore the feature space through branching trajectories. Each branch's extension follows golden ratio proportions, ensuring efficient coverage of the high-dimensional search space while maintaining mathematical elegance in the exploration strategy.

The Fibonacci principles manifest in multiple algorithmic components: the population sizing follows Fibonacci numbers to balance diversity and computational efficiency; the branch length ratios use golden ratio scaling to create hierarchical search resolution; and the convergence criterion employs Fibonacci sequence properties to detect algorithmic stagnation. Experimental evaluations across

diverse machine learning benchmarks—including biomedical diagnosis datasets, financial time series prediction problems, and image classification tasks—demonstrate that GLA identifies feature subsets 10-30% smaller than those found by conventional wrapper methods while maintaining or improving predictive accuracy.

Particularly noteworthy is GLA's performance on imbalanced classification problems where minority class representation is critical. The algorithm's exploration strategy naturally discovers feature combinations that enhance minority class discrimination, achieving F1-score improvements of 5-15% compared to recursive feature elimination and forward selection approaches. This capability has driven adoption in medical diagnosis applications, fraud detection systems, and rare event prediction scenarios where feature selection quality directly impacts decision-making reliability.

Wireless Sensor Networks

Yang and collaborators (2023) developed an innovative jammer location-aware methodology based on Fibonacci branch search principles for enhancing security in wireless sensor networks (WSNs). Jamming attacks—where malicious actors transmit interference signals to disrupt network communications—pose serious threats to WSN applications in critical infrastructure monitoring, military operations, and industrial control systems. Rapid and accurate jammer localization enables effective countermeasures such as adaptive channel hopping, power control, or physical jammer neutralization.

The jammer localization problem presents significant algorithmic challenges due to the irregular propagation characteristics of jamming signals in complex environments with obstacles, multipath effects, and shadowing. Traditional localization approaches based on received signal strength (RSS) measurements suffer from ambiguity, as multiple potential jammer positions may produce similar RSS patterns across the sensor network. The Fibonacci branch search methodology addresses this ambiguity through systematic exploration of the geographical search space, progressively narrowing the possible jammer location region.

The algorithm constructs a hierarchical spatial partition where each partition level follows Fibonacci sequence ratios, creating increasingly refined location hypotheses. At each search iteration, the method evaluates candidate jammer positions by predicting their expected RSS footprint across the sensor network and comparing these predictions to actual measurements. The branch selection strategy prioritizes regions showing the best measurement-prediction agreement while maintaining backup branches in alternative regions to avoid premature convergence.

Field experiments in urban environments with 50-200 sensor nodes have demonstrated that the Fibonacci branch search approach localizes jammers with median position errors of 2-4 meters, representing 40-60% improvement over centroid-based and least-squares localization methods. The algorithm exhibits particular robustness to sensor node failures and incomplete measurements—common conditions during active jamming attacks. Response times typically range from 3-8 seconds depending on network size, enabling rapid deployment of countermeasures. This performance profile has led to implementation in several defense-related WSN deployments and critical infrastructure protection systems where jamming resilience is a primary security requirement.

These diverse applications collectively demonstrate that Fibonacci search methods, far from being purely theoretical constructs, provide practical computational advantages across a remarkable spectrum of engineering disciplines. The continued development and adaptation of these techniques suggests their sustained relevance in addressing emerging optimization challenges in an increasingly complex technological landscape.

7.4. Trisection Method with k-Lucas Numbers

Demir (2008) developed a trisection method using k-Lucas numbers based on the bisection method for finding roots of nonlinear equations. This approach eliminates disadvantages of the classical

bisection method and demonstrates faster convergence. The trisection method divides the search interval into three parts rather than two, using k-Lucas number ratios to determine the division points.

7.5. Integration with Artificial Intelligence and Machine Learning

Recent research has explored the integration of Fibonacci and golden ratio concepts with artificial intelligence and machine learning. The golden ratio optimization method (GROM), proposed as a parameter-free meta-heuristic optimization algorithm, is inspired by the golden ratio found in plant and animal growth patterns. This method employs the golden ratio to update solutions in optimization algorithms without requiring parameter tuning.

Studies have also investigated using Fibonacci numbers for neural network weight initialization and the golden ratio as a learning rate, with some researchers reporting improved learning curve performance. While this remains an experimental area, it suggests potential connections between natural mathematical patterns and artificial intelligence optimization.

Youvan (2024) explored leveraging the golden ratio and Fibonacci sequence for optimized AI decision-making, proposing theoretical frameworks for incorporating these mathematical concepts into AI algorithms for navigation, resource allocation, and planning applications.

8. Conclusions and Future Directions

In one-dimensional optimization, the Fibonacci search method stands as one of the most efficient algorithms for finding optimal points of unimodal functions. This chapter has presented comprehensive improvements on the classical Fibonacci search algorithm using Lucas numbers and k-Lucas numbers, demonstrating significant enhancements in convergence speed and accuracy.

The key findings from this study can be summarized as follows:

1. Using Lucas numbers instead of Fibonacci numbers in the search algorithm provides faster convergence to optimal points, particularly for smaller iteration numbers.
2. The generalization to k-Lucas numbers offers additional flexibility and can provide even better results for certain problem types.
3. The lengths of final intervals computed by the improved methods are smaller than those from the classical Fibonacci search for the same number of iterations.
4. The optimal values of objective functions are more accurate in the improved methods.
5. The improvements are most significant for practical applications where computational resources limit the number of function evaluations.

These improvements have significant implications for multivariate optimization methods such as Powell's method, which rely on one-dimensional search algorithms to converge to optimum points. Since the improved methods converge more rapidly and provide more accurate objective function values, they can make crucial contributions to such methods, especially when applied to large-scale optimization problems where computational efficiency is paramount.

Future research directions include further exploration of the parametrized approaches, development of adaptive methods that automatically select optimal k values, and integration with modern meta-heuristic and machine learning optimization techniques. The continued relevance of these methods, as demonstrated by recent applications in structural health monitoring, wireless communications, and artificial intelligence, suggests that Fibonacci-type search methods will remain important tools in the optimization toolkit for years to come.

References

[1] Yıldız, B., & Karaduman, E. (2003). On Fibonacci search method with k-Lucas numbers. *Applied Mathematics and Computation, 143*, 523-531.

[2] Subaşı, M., Yıldırım, N., & Yıldız, B. (2004). An improvement on Fibonacci search method in optimization theory. *Applied Mathematics and Computation, 147*, 893-901.

[3] Demir, A., Ömür, N., & Ulutaş, Y.T. (2008). Optimization by k-Lucas numbers. *Applied Mathematics and Computation, 197*, 366-371.

[4] Demir, A. (2008). Trisection method by k-Lucas numbers. *Applied Mathematics and Computation, 198*, 339-345.

[5] Ömür, N., Demir, A., & Ulutaş, Y.T. (2008). Parametrized Fibonacci search method with k-Lucas numbers. *Applied Mathematics and Computation, 201*, 719-727.

[6] Chong, C.Y., Leow, S.K., & Sim, H.S. (2021). Generalized Fibonacci Search Method in One-Dimensional Unconstrained Non-Linear Optimization. *Pertanika Journal of Science and Technology, 29*(2), 1017-1039.

[7] Tran-Ngoc, H., et al. (2023). A promising approach using Fibonacci sequence-based optimization algorithms and advanced computing. *Scientific Reports, 13*, 3405.

[8] Rahman, M.S., & Shaikh, A.A. (2023). Extensions of Fibonacci Search Technique for One Dimensional Interval Optimization Problem. *Computational Methods in Applied Mathematics*.

[9] Yang, F., et al. (2023). Jammer Location-Aware Method in Wireless Sensor Networks Based on Fibonacci Branch Search. *Journal of Sensors, 2023*.

[10] Pereira, J.L.J., et al. (2024). Golden Lichtenberg algorithm: a Fibonacci sequence approach applied to feature selection. *Neural Computing and Applications*.

[11] Implementation of a novel Fibonacci branch search optimizer for adaptive beamformer design. (2020). *International Journal of Microwave and Wireless Technologies, 12*(7), 625-634.

[12] Youvan, D.C. (2024). Leveraging the Golden Ratio and Fibonacci Sequence for Optimized AI Decision-Making. *ResearchGate Preprint*.

[13] Kiefer, J. (1953). Sequential minimax search for a maximum. *Proceedings of the American Mathematical Society, 4*, 502-506.

[14] Gill, P.E., Murray, W., & Wright, M.H. (1981). *Practical Optimization*. Academic Press, London.

[15] Sivazlian, B.D., & Stanfel, L.E. (1975). *Optimization Techniques in Operations Research*. Prentice-Hall, New Jersey.

[16] Lee, G.Y. (2000). k-Lucas numbers and associated bipartite graphs. *Linear Algebra and its Applications, 320*, 51-61.

[17] Ratz, D. (1999). A nonsmooth global optimization technique using slopes: the one-dimensional case. *Journal of Global Optimization, 14*(4), 365-393.

[18] Törn, A., & Žilinskas, A. (1989). *Global Optimization*. Lecture Notes in Computer Science, No. 350, Springer-Verlag.

[19] Koshy, T. (2019). *Fibonacci and Lucas Numbers with Applications*. John Wiley & Sons.

[20] Bazaraa, M.S., Sherali, H.D., & Shetty, C.M. (2013). *Nonlinear Programming: Theory and Algorithms*. 3rd ed., John Wiley & Sons.

[21] Hosseini, S., & Al Khaled, A. (2019). A novel meta-heuristic optimization method based on golden ratio in nature. *Soft Computing, 23*, 8979-8998.

Chapter 2

ON SPACELIKE CURVES WITH Q-FRAME HAVING TIMELIKE NORMAL, SPACELIKE BINORMAL IN 3-DIMENSİONAL MINKOWSKI SPACE

Rabia Kalmuk[1]

1 Kocaeli University Institute of Science, Department of Mathematics, İzmit-Kocaeli, Türkiye (ORCID: 0009-0009-0890-792X) klmkrabia@gmail.com

INTRODUCTION

Curves called rectifying are defined as space curves that lie on the rectifying plane spanned by binormal and tangent vector fields in 3-dimensional Euclidean space, as studied in [9]. Moreover, in the same study, a simple classification is provided for these types of curves defined by B. Y. Chen. Particularly, it is proven in study [11] that rectifying curves are related with centrodes, which are significant on kinematics and mechanics. It also corresponds a non-constant function of a regular curve [10]. In addition, timelike and spacelike curves in Minkowski three-space are studied by means of the concept of centrode [15, 17, 18].

Suppose c(t) is the position vector of a rectifying curve in IR^3. Then, the position vector can be given with the help of the Frenet vectors as

$$c(t) = f_1(t)e_1(t) + f_3(t)e_3(t). \tag{1}$$

Here, $f_1(t)$ and $f_3(t)$ are smooth functions.

Frenet frame is used for curves which can be differentiate and non-degenerate. This means that the second derivative of the related curve can vanish. Therefore, we need a new frame [1].

Q-frame is more useful compared to other frames (Frenet, Bishop etc.) [1, 20, 23]. To give an example, Q- frame is also defined on a straight line. There is no more difference on Q-frames for a unit speed curve and non-unıt speed curve, and they are determined easily [14].

The position vector c(t) for a regular curve can be analyzed as the sum of normal component and tangent component:

$$c = c^T + c^N. \tag{2}$$

If $\dfrac{\|c^T\|}{\|c^N\|}$ is equal to a real constant, then these types of curves are known as constant ratio curves [8].

Here, $\|c^T\|$ and $\|c^N\|$ are the length of the vectors c^T and c^N, respectively. As it is understood that this definition also corresponds to constancy of the ratio $\dfrac{\|c^T\|}{\|c\|}$ [2,3,4,5,6,7,21,22,24,25,28,29].

Particularly, since the expression $\|grad(\|c\|)\|$ is also equal to mentioned ratio, satisfying the relation

$$\|grad(\|c\|)\| = L, \quad L \text{ const.} \tag{3}$$

means that the curve has constant ratio [8].

In this work, a spacelike curve in Minkowski three- space is handled as a linear combination of Q-frame:

$$c(t) = f_1(t)e_1(t) + f_2(t)e_2(t) + f_3(t)e_3(t) \tag{4}$$

In this equality, $f_i(t), i = 1,2,3$ are curvature functions and $e_i(t), i = 1,2,3$ are Q- frame vector fields.

We examine when a unit speed spacelike curve corresponds to constant ratio, N- constant or T-constant curve [19].

1.PRELIMINARIES

Suppose, pseudo-Euclidean space with 1 index is represented by IR_1^3. Then, the inner product (Lorentz) is defined as

$$\langle q, r\rangle_L = -q_1r_1 + q_2r_2 + q_3r_3. \tag{5}$$

Here, the vector fields are $q = (q_1, q_2, q_3)$, $r = (r_1, r_2, r_3) \in IR_1^3$.

$S_1^2(d^2)$ and $H_0^2(-d^2)$ are known as pseudo-Riemann and pseudo-hyperbolic spaces, respectively and the related sets are

$$S_1^2(d^2) = \{q \in IR_1^3 : \ \langle q, q\rangle_L = d^2\} \tag{6}$$

and

$$H_o^2(-d^2) = \{r \in IR_1^3 : \ \langle r, r\rangle_L = -d^2\}, \tag{7}$$

where d is positive constant. Particularly, $H_0^2(-d^2)$ and $S_1^2(d^2)$ are also called as anti de-Sitter space-time and Sitter space-time [12].

Recall that, for $q \in IR_1^3$, if $\langle q, q\rangle_L < 0$ or $\langle q, q\rangle_L > 0$ or $\langle q, q\rangle_L = 0 \quad (q \neq 0)$, then the vector is said to be timelike, spacelike or lightlike, respectively. The norm of q is

$$\|q\| = \sqrt{|\langle q, q\rangle|}. \tag{8}$$

In case of being $\langle q, r\rangle_L = 0$, the orthogonality occurs. In addition to this, an arbitrary curve $c(t)$ in IR_1^3 is said to be timelike, spacelike or null, if the velocity vector $c'(t)$ is timelike, spacelike or null respectively [26].

In case $\langle c'(t), c'(t)\rangle_L = \pm 1$ for the timelike or spacelike curve, it has unit speed. The set of lightlike cone $\mathbb{L}C$ in IR_1^n can be written by

$$\mathbb{L}C = \{q \in IR_1^n, \quad \langle q, q\rangle_L = 0\}.$$

Assume that, $c : J \subset IR \to IR_1^3$, is a unit speed curve in 3-Minkowski space. Then, $c'(t) = e_1(t)$ is congruent to the unit tangent vector and the first Frenet curveture is $K_1(t) = \|c''(t)\|$. If $K_1(t)$ don't vanish, the normal vector satisfy $e_2'(t) + K_1(t)e_1(t) = K_2(t)e_2(t)$. Here, $K_2(t)$ is the torsion which is the second Frenet curvature. If $K_2(t)$ doesn't vanish, for binormal vector $e_3(t)$, the equality $e_3'(t) = -K_2(t)e_2(t)$ is valid. Therefore, the vectors Frenet-Serret are

$$\begin{aligned} e_1'(t) &= \epsilon_1 K_1(t)e_2(t), \\ e_2'(t) &= -\epsilon_1 K_1(t)e_1(t) - \epsilon_1\epsilon_2 K_2(t)e_3(t), \\ e_3'(t) &= -\epsilon_2 K_2(t)e_2(t). \end{aligned} \tag{9}$$

Here

$$\epsilon_1 = \langle e_1(t), e_1(t)\rangle_L = \pm 1 \quad \epsilon_2 = \langle e_2(t), e_2(t)\rangle_L = \pm 1, \ \epsilon_3 = \langle e_3(t), e_3(t)\rangle_L = -\epsilon_1\epsilon_2 ,$$

[27].

Q-frame of the space curve c(t) have three orthonormal vector fields. They are the tangent vector $e_1(t)$, q-normal $e_2(t)$, q-binormal $e_3(t)$ and determined as

$$e_1 = \frac{c'}{\|c'\|},$$

$$e_2 = \frac{e_1 \times k}{\|e_1 \times k\|} \tag{10}$$

$$e_3 = e_1 \times e_2$$

Here, the projection vector is denoted by k and it is on x-axis, y-axis or z-axis [13].

The q-frame's derivative formulas are not related with k vector being spacelike or timelike. Thus, the projection vector can be chosen spacelike.

If a chosen curve is spacelike, then we know that tangent vector is spacelike. In addition, one of the normal vector and the binormal vector must be timelike. We set timelike vector is the normal vector field of c(t). Therefore, the matrix of the derivative formula is

$$\begin{bmatrix} e_1' \\ e_2' \\ e_3' \end{bmatrix} = \begin{bmatrix} 0 & K_1 & -K_2 \\ K_1 & 0 & K_3 \\ K_2 & K_3 & 0 \end{bmatrix} \begin{bmatrix} e_1 \\ e_2 \\ e_3 \end{bmatrix}. \tag{11}$$

where
$K_1 = \kappa \cosh\alpha$, $K_2 = \kappa \sinh\alpha$, and $K_3 = \tau + \alpha'$ are q-curvatures of c(t) [14].

2. THE EVALUATION OF CURVES IN ACCORDANCE WITH Q-FRAME IN 3-MINKOWSKI SPACE

In this part, we evaluate the spacelike curves having timelike normal, spacelike binormal according to Q-frame given by the parameter t in IR_1^3. Suppose that $c : J \subset IR \to IR_1^3$ is defined as a unit speed curve with the principle curvatures K_1, K_2, K_3. Based on the definition, the position vector c satisfy the equation (4) where $f_i(t), 0 \le i \le 2$ are curvature functions. By differentiating (4), it is handled that

$$c(t) = f_1'(t)e_1(t) + f_1(t)e_1'(t) + f_2'(t)e_2(t) + f_2(t)e_2'(t) + f_3'(t)e_3(t) + f_3(t)e_3'(t)$$

and by using (11) one can write

$$\begin{aligned} c'(t) = {} & (f_1'(t) + K_1(t)f_2(t) + K_2(t)f_3(t))e_1(t) \\ & + (f_2'(t) + K_1(t)f_1(t) + K_3(t)f_3(t))e_2(t) \\ & + (f_3'(t) - K_2(t)f_1(t) + K_3(t)f_2(t))e_3(t). \end{aligned} \tag{12}$$

Since $c(t)$ is a unit speed curve (i.e $c'(t) = e_1(t)$), the following lemma is encountered.

Lemma: Let $c : J \subset IR \to IE_1^3$ be a spacelike curve having timelike normal, spacelike binormal given by the vectorial equation (4). Then, the system

$$f_1' + K_1 f_2 + K_2 f_3 = 1$$

$$f_2' + K_1 f_1 + K_3 f_3 = 0 \tag{13}$$

$$f_3' - K_2 f_1 + K_3 f_2 = 0$$

is satisfied, where K_1, K_2, K_3 are the Q-curvatures of $c(t)$.

Corollary: Let $c : J \subset IR \to IE_1^3$ be a spacelike W- curve having timelike normal, spacelike binormal. Then, the relation between the curvature functions is given by the differential equation

$$f_1'' = \left(K_1^2 - K_2^2\right) f_1 + K_3\left(K_1 f_3 + K_2 f_2\right)$$

Proof: Let $c(t)$ be a spacelike W- curve given by the vectorial equation (4). Then, the principle curvatures are constant functions. Differentiating the first equation of (13), we get

$$f_1'' = -\left(K_1 f_2' + K_2 f_3'\right) \tag{14}$$

With the help of the second and the third equation of (13), we arrange (14) and obtain the desired result.

2.1.Spacelike Constant Ratio Curves with Quasi Frame

Definition: Let $c : J \subset IR \to IE_1^3$ be a curve that is non-lightlike and parameterized by arc-length. The position vector of the curve can be expressed as a linear combination of its normal and tangential components so as to satisfy equation (2). If the ratio $\dfrac{\left\|c^T\right\|}{\left\|c^N\right\|}$ is constant along c(I), the curve is called a constant-ratio curve[8]. It is known that the constancy of this ratio is equivalent to to the constancy of $\dfrac{\left\|c^T\right\|}{\|c\|}$. Denote this constant ratio by L. Since $\|c\| = L.t$, it follows that

$$\begin{aligned} &\frac{\left\|c^T\right\|}{L.t} = L, \\ &\left\|c^T\right\| = L^2.t. \end{aligned} \tag{15}$$

Theorem: Let $c : J \subset IR \to IE_1^3$ be a spacelike unit speed curve having timelike normal, spacelike binormal, defined by vectorial equation (4). If c has constant ratio, then its parameterization is given by

$$\begin{aligned} c(t) = (L)^2 t\, e_1(t) &+ \frac{K_1\left(L^2 - 1\right) \pm K_2\sqrt{\left(K_1^2 - K_2^2\right)\left(1 - L^2\right)L^2 t^2 + \left(1 - L^2\right)^2}}{K_2^2 - K_1^2} e_2(t) \\ &+ \frac{K_2\left(1 - L^2\right) \pm K_1\sqrt{\left(K_1^2 - K_2^2\right)\left(1 - L^2\right)L^2 t^2 - \left(1 - L^2\right)^2}}{K_2^2 - K_1^2} e_3(t). \end{aligned} \tag{16}$$

Proof: Assume that $c : J \subset IR \to IE_1^3$ be a spacelike unit speed curve, defined by vectorial equation (4). Then, equation system (13) is hold. If the related curve is of constant ratio, we have

$$f_1(t) = (L)^2 t$$

and (17)

$$f_1'(t) = L^2.$$

dir. Substituting (17) into the first equation of (13), we get

$$f_3 = \frac{(1 - L^2) - K_1 f_2}{K_2}. \tag{18}$$

Moreover, by multiplying the second and third equation of (13) with f_2 and f_3 respectively, and then adding them together, we obtain

$$f_2^2 - f_3^2 = L^2 t(L^2 - 1), \tag{19}$$

and using (18) we get

$$f_2 = \frac{K_1(L^2 - 1) \pm K_2\sqrt{(K_1^2 - K_2^2)(1 - L^2)L^2 t^2 + (1 - L^2)^2}}{K_2^2 - K_1^2}.$$

Similarly, we write

$$f_3 = \frac{K_2(1 - L^2) \pm K_1\sqrt{(K_1^2 - K_2^2)(1 - L^2)L^2 t^2 - (1 - L^2)^2}}{K_2^2 - K_1^2}.$$

Hence, writting these curvature functions into the vectorial equation (4), we obtain (16) and this completes the proof.

2.2. Spacelike T-Constant Curves with Quasi Frame

Definition: Let $c : J \subset IR \to IE_1^3$ be a curve that is non-lightlike and parameterized by arc-length.If $\|c^T\|$ remains constant, the curve is referred to as a T-constant curve [9]. Additionally, if $\|c^T\| = 0$, the curve is called a T-constant curve of first type, and in the other case, it is referred to as a T-constant curve of secont type [16]. Based on the equations (4) and (13), we can state the following Lemma:

Lemma: Let $c : J \subset IR \to IE_1^3$ be a spacelike unit speed curve having timelike normal, spacelike binormal, defined by vectorial equation (4). c(t) is a T-constant curve of first type if and only if

$$K_1 f_2 + K_2 f_3 = 1,$$

$$f_2' = -K_3 f_3, \tag{20}$$

$$f_3' = -K_3 f_2.$$

Theorem: : Let $c : J \subset IR \to IE_1^3$ be a spacelike unit speed curve having timelike normal, spacelike binormal, defined by vectorial equation (4). If c(t) is a T-constant curve of first type, then its parametrization is

$$c(t) = \frac{-K_1 \pm K_2\sqrt{\left(K_2^2 - K_1^2\right)\ell + 1}}{K_1^2 - K_2^2} e_2(t) + \frac{-K_2 \pm K_1\sqrt{\left(K_2^2 - K_1^2\right)\ell + 1}}{K_1^2 - K_2^2} e_3(t). \tag{21}$$

Proof: Assume, $c : J \subset IR \to IE_1^3$ be a spacelike unit speed curve having timelike normal, spacelike binormal. Then, the system (13) is satisfied. If the curve is a T-constant curve of first type, it follows from the definition that

$$f_1(t) = 0.$$

From the first equation of the system (20), we obtain

$$f_3 = \frac{1 - K_1 f_2}{K_2}. \tag{22}$$

Furthermore, by multiplying the second and the final equations of the system (13) by f_2 and f_3, respectively, and adding these two equations, we get,

$$f_2^2 - f_3^2 = \ell \tag{23}$$

where ℓ is real constant. Using equation (22), one can derive

$$f_2 = \frac{-K_1 \pm K_2\sqrt{\left(K_2^2 - K_1^2\right)\ell + 1}}{K_1^2 - K_2^2}. \tag{24}$$

Consequently, in a similar manner,

$$f_3 = \frac{-K_2 \pm K_1\sqrt{\left(K_2^2 - K_1^2\right)\ell + 1}}{K_1^2 - K_2^2} \tag{25}$$

holds. Due to the vectorial equation (4), the parameterization given by (21) is obtained, and the proof is complete.

From the curvature functions (24) and (25), and the final equation of the system (20), the following result can be derived.

Teorem: : Let $c : J \subset IR \to IE_1^3$ be a spacelike unit speed curve having timelike normal, spacelike binormal, defined by vectorial equation (4). If c(t) is a T-constant curve of first type, then its Q-curvatures satisfy the relation

$$\left(\frac{-K_1 \pm K_2\sqrt{\left(K_2^2 - K_1^2\right)\ell + 1}}{K_1^2 - K_2^2}\right)' = -K_3\left(\frac{-K_2 \pm K_1\sqrt{\left(K_2^2 - K_1^2\right)\ell + 1}}{K_1^2 - K_2^2}\right) \tag{26}$$

Lemma: Let $c : J \subset IR \to IE_1^3$ be a spacelike unit speed curve having timelike normal, spacelike binormal, defined by vectorial equation (4). Then c(t) is a T-constant curve of second type if and only if the system

$$\begin{aligned} &K_1 f_2 + K_2 f_3 = 1, \\ &f_2' + K_1 \ell + K_3 f_3 = 0, \\ &f_3' - K_2 \ell + K_3 f_2 = 0, \end{aligned} \tag{27}$$

is hold where ℓ is real constant.

Theorem: Let $c : J \subset IR \to IE_1^3$ be a spacelike unit speed curve having timelike normal, spacelike binormal, defined by vectorial equation (4). If c(t) is a T-constant curve of second type, then the relation between curvature functions is

$$f_2^2 - f_3^2 = 2\ell.t + d, \tag{28}$$

where $\ell, d \in IR$.

Proof: Assume, $c(t)$ is a spacelike T-constant curve of second type in IE_1^3. Then, the system (28) is hold. By multiplying the 2. eq. and 3. eq. with f_2 and f_3, we see the sum of these is

$$f_2 f_2' - f_3 f_3' = -\ell. \tag{29}$$

By integrating (29), one can obtain (28) and complete the proof.

Theorem: : Let $c : J \subset IR \to IE_1^3$ be a spacelike unit speed curve having timelike normal, spacelike binormal, defined by vectorial equation (4). If c(t) is a T-constant curve of second type, then its representation is

$$c(s) = \ell.\, e_1(t) + \frac{-K_1 \pm K_2\sqrt{(K_2^2 - K_1^2)(-2\ell.t + d) + 1}}{K_2^2 - K_1^2} e_2(t) + \frac{K_2 \pm k_1\sqrt{(K_2^2 - K_1^2)(-2\ell.t + d) + 1}}{K_2^2 - K_1^2} e_3(t)$$

Proof: Assume, $c(t)$ is a spacelike T-constant curve of second type in IE_1^3. Then, the system (27) is hold. From the 1. eq. of the system (27), we write

$$f_3 = \frac{1 - K_1 f_2}{K_2} \tag{30}$$

Substituting (30) into (28), we find

$$f_2 = \frac{-K_1 \pm K_2\sqrt{(K_2^2 - K_1^2)(-2\ell.t + d) + 1}}{K_2^2 - K_1^2} \tag{31}$$

and similarly

$$f_3 = \frac{K_2 \pm k_1\sqrt{(K_2^2 - K_1^2)(-2\ell.t + d) + 1}}{K_2^2 - K_1^2}. \tag{32}$$

Substituting these into the vectorial equation (4), we complete the proof.

2.2. Spacelike N-Constant Curves with Quasi Frame

Definition: Let $c : J \subset IR \to IE_1^3$ be a curve that is non-lightlike and parameterized by arc-length.If $\left\|c^N\right\|$ remains constant, the curve is referred to as a N-constant curve [9]. Additionally, if $\left\|c^N\right\| = 0$, the curve is called a N-constant curve of first type, and in the other case, it is referred to as a N-constant curve of secont type [16]. Based on the equations (4) and (13), we can state the following Lemma:

In case of the spacelike curve having a timelike normal, a spacelike binormal, and being N-constant, it is clear from the Lorentzian inner product of its normal component with itself that

$$\left\|c^N\right\|^2 = -(f_2)^2 + (f_3)^2 = \ell. \tag{33}$$

Differentiating equation (33) in conjunction with system (13) allows us to state the following Lemma:

Lemma: Let $c : J \subset IR \to IE_1^3$ be a spacelike unit speed curve having timelike normal, spacelike binormal. Then, $c(t)$ is a N-constant if and only if

$$\begin{aligned} &f_1' + K_1 f_2 + K_2 f_3 = 1, \\ &f_2' + K_1 f_1 + K_3 f_3 = 0, \\ &f_3' - K_2 f_1 + K_3 f_2 = 0, \\ &-f_2 f_2' + f_3 f_3' = 0 \end{aligned} \tag{34}$$

is hold.

Theorem: : Suppose that $c : J \subset IR \to IE_1^3$ is a spacelike unit speed curve having timelike normal, spacelike binormal and N-constant curve of second type. Then, $c(t)$ is congruent to a T-constant curve of first type with the parameterizations

$$c(s) = \frac{1}{K_1 + K_2}\left(e_2(t) + e_3(t)\right) \tag{35}$$

$$c(s) = \frac{1}{K_1 - K_2}\left(e_2(t) - e_3(t)\right) \tag{36}$$

or the curvature functions satisfy

$$\begin{aligned} &f_1(t) = t + d, \\ &f_i(t) - K_3 f_i + K_1 t = 0, \ i = 2,3. \end{aligned}$$

Proof: Assume, the curve $c(t)$ is a spacelike N-constant curve of first kind. Then,

$$-(f_2)^2 + (f_3)^2 = 0.$$

Hence, we know $f_2 = f_3$ or $f_2 = -f_3$. Substituting these into the system (34), we obtain

$$(K_1 + K_2)f_1 = 0$$

or

$$(K_1 - K_2)f_1 = 0.$$

Therefore, if $f_1 = 0$, then the curve corresponds to a T-constant curve of first type and

$$f_i(t) = \frac{1}{K_1 \pm K_2} \; ; \; i = 2, 3$$

$$f_i(t) = \frac{1}{K_1 + K_2}$$

If $K_1 = \pm K_2$, then, with the help of the system (34), we yield

$$f_1(t) = t + d,$$
$$f_i(t) - K_3 f_i + K_1 . t = 0, \; i = 2,3.$$

This completes the proof.

Theorem: : Let $c : J \subset IR \to IE_1^3$ be a spacelike unit speed curve having timelike normal, spacelike binormal and N-constant curve of second type. Then, $c(t)$ is congruent to a T-constant curve of first type or it has the curvature function

$$f_1(t) = t + d, \tag{37}$$

where d is a real constant.

Proof: Assume, the curve $c(t)$ is a spacelike N-constant curve of second kind. Then, the system (34) is hold. Multiplying the 2. Eq. and 3. Eq. with $-f_2$ and f_3, respectively. Further, taking sum of these equalities we get

$$f_1(K_1 f_2 + K_2 f_3) = 0.$$

In case of being $f_1(t) = 0$, then this means that the curve $c(t)$ corresponds to a T-constant curve of first type. In case of being

$$K_1 f_2 + K_2 f_3 = 0,$$

then using the 1. Eq of the system (34) we yield $f_1'(t) = 1$ which means that the curvature function $f_1(t)$ is given by (37). This completes the proof.

3. REFERENCES

[1] Bayram, B. K., Önen, N., Curves of restricted type in Euclidean spaces, Mathematica Moravica, 2014, Vol. 18,(1) 89-98.

[2] Büyükkütük, S., A new approach to timelike hypersurfaces of constant ratio in E_1^4, Journal of Mathematics, 2023, Vol. 2023, Article ID 8495667.

[3] Büyükkütük, S., Öztürk G., Constant ratio curves according to Bishop frame in Euclidean 3-space E^3, Gen. Math. Notes, 2015, Vol. 28(1), 81-91.

[4] Büyükkütük, S., Öztürk G., Constant ratio curves according to parallel transport frame in Euclidean 4-space E^4, New Trends in Mathematical Sciences, 2015, Vol. 3(4), 171-178.

[5] Büyükkütük, S., Kişi İ., Mishra, V.N., Öztürk G., Some characterizations of curves in Galilean 3-space G3, Facta Universitatis Series: Mathematics and Informatics, 2016, Vol. 31(2), 503-512.

[6] Büyükkütük, S., Kişi İ., Öztürk G., A characterization of non-lightlike curves with respect to paralel transport frame in Minkowski space-time, Malaysian Journal of Mathematical Sciences, 2018, Vol. 12(2), 223-234.

[7] Büyükkütük, S., Kişi İ., Öztürk G., Arslan, K., Some characterizations of curves in n-dimensional Euclidean space, Iğdır Üniversitesi Fen Bilimleri Dergisi, 2020, Vol. 10(2), 1273-1285.

[8] Chen, B.Y., Constant-ratio hypersurfaces, Soochow Journal of Mathematics, 2001, Vol. 27, 353-362.

[9] Chen, B. Y., Convolution of Riemannian manifolds and its applications, Bull. Aust. Math. Soc., 2002, Vol. 66(2), 177–191.

[10] Chen, B.Y., When does the position of a space curve always lies in its rectifying plane?, Amer. Math. Monthly, 2003, Vol. 110, 147-152.

[11] Chen,B. Y. and Dillen, F., Rectifying curves as centrodes and extremal curves, Bull. Inst. Math. Academia Sinica, 2005, Vol. 33, 77-90.

[12] Dugal,, K. L., Bejancu, A., Lightlike submanifolds of Semi-Riemann manifolds and applications, Kluwer Academic, Dordrecht, 1996.

[13] Ekici C., Göksel, M.B.., Dede, M., Smarandache curves according to q-frame in Minkowski 3-space, Conference Proceedings of Science and Technology, 2019, Vol. 2(2), 110–118.

[14] Elsayied, H.K., Tawfiq, A. M and Elsharkawy, A., The quasi frame and equations of non-lightlike curves in Minkowski E_1^3 and E_1^4, Italian Journal of Pure and Applied Mathematics, 2023, Vol. 49, 225-239.

[15] Ezentaş, R., Türkay, S., Helical versus of rectifying curves in Lorentzian spaces, Dumlupınar Üniv. Fen Bilim. Enst. Dergisi, 2004, Vol. 6, 239-244.

[16] Gürpınar, S., Arslan, K., Öztürk, G., A characterization of constant ratio curves in Euclidean 3-space, Acta Universtatis Apulensis, 2015, Vol. 44, 39–51.

[17] İlarslan, K., Nesovic, E. and Petrovic, T. M., Some characterizations of rectifying curves in the Minkowski 3-space, Novi. Sad. J. Math., 2003, Vol. 32, 23–32.

[18] İlarslan, K. and Nesovic, E., On rectifying curves as centrodes and extremal curves in the Minkowski 3-space IE_1^3, Novi. Sad. J. Math., 2007, Vol. 37, 53–64.

[19] Kalmuk, R. (2025), A Classification of Constant Ratio Curves with respect to Quasi Frame, (Master's thesis, Kocaeli University).

[20] Kalmuk, R., Büyükkütük, S., Öztürk G., Curves of constant ratio with quasi frame in E^3, Turkish Journal of Nature and Science, 2024, Vol. 1, 103–108.

[21] Kişi, İ., Öztürk, G., A new characterization of curves in Minkowski 4-space E_1^4, Facta Universitatis Ser. Math. Inform., 2020, Vol. 35(1), 187–199.

[22] Kişi, İ., Öztürk, G., Constant ratio curves according to Bishop frame in Minkowski 3-space, Facta Universitatis Ser. Math. Inform., 2015, Vol. 30, 527–538.

[23] Kişi İ., Büyükkütük, S., Deepmala, Öztürk G., AW(k)-type curves according to parallel transport frame in Euclidean space E^4, Facta Universitatis Series: Mathematics and Informatics, 2016, Vol. 31(4), 885-905.
[24] Kişi, İ., Büyükkütük, S., Öztürk, G., Zor, A., A new characterization of curves on dual unit sphere, Journal of Abstract and Computational Mathematics, 2017, Vol. 2(1), 71-76.
[25] Kişi, İ., Büyükkütük, S., Öztürk, G., Constant ratio timelike curves in pseudo-Galilean 3-space G_1^3, Creative Mathematics and Informatics, 2018, Vol. 27(1), 57–62.
[26] O'Neill, B., Semi-Riemannian Geometry with applications to relativity, Pure and Applied Mathematics, Academic Press, 1983.
[27] Özdemir, M., Erdoğdu, M., Şimşek, H., Ergin, A.A., Backlund transformation for spacelike curves in the Minkowski space-time, Kuwait J. Sci., 2014, Vol. 41, 63-80.
[28] Öztürk,, G., Büyükkütük, S., Kişi, İ., A characterization of curves in Galilean 4-space G_4, Bulletin of Irannian Mathematical Society, 2017, Vol. 43(3), 771-780.
[29] Öztürk,, G., Kişi, İ., Büyükkütük, S., Constant ratio quaternionic curves in Euclidean spaces,Advances in Applied Clifford Algebras, 2017, Vol. 27(2), 1659-1673.

Chapter 3

UNRESTRICTED PELL AND PELL-LUCAS 3-PARAMETER GENERALIZED QUATERNIONS

Göksal BİLGİCİ[1]

1 Prof. Dr., Kastamonu University, Faculty of Education, Department of Elementary Mathematics Education

E-mail: gbilgici@kastamonu.edu.tr, ORCID: 0000-0001-9964-5578

1. INTRODUCTION

The Pell and Pell-Lucas sequences are two sequences among the most renowned integer sequences. Both sequences manifest in abstract mathematics as well as in diverse applied domains such as Pell equations, algebraic number theory, and computer science (Koshy, 2014). Both sequences emerge organically while examining units in the quadratic integer ring $\mathbb{Z}[\sqrt{2}]$. The unit $1+\sqrt{2}$ gives all solutions to $x+y\sqrt{2}=\left(1+\sqrt{2}\right)^n$. The coefficients of this expansion yield Pell–Lucas and Pell numbers. Pell numbers are relevant in issues concerning rational approximations of diagonal slopes, near-integer solutions for right triangles with irrational ratios, and scaled approximations of isosceles triangles with side lengths related by $\sqrt{2}$. Pell numbers are essential for approaching quadratic irrationals, akin to how Fibonacci numbers approximate the golden ratio.

Pell numbers enumerate several combinatorial entities. The number P_n enumerates ways to tile a $1\times n$ board with: "dominoes" of length 2 (weight 1) and "monominoes" of length 1 (weight 2). The quantity of binary strings of length n with: no occurrence of pattern "00" and weight rules for allowed concatenations yields the Pell sequence.

These sequences adhere to the following identical second-order recursive connection

$$U_n=2U_{n-1}+U_{n-2} \tag{1.1}$$

except the initial conditions. The initial conditions of the Pell sequence $\{P_n\}$ are $P_0=0$ and $P_1=1$, whereas the initial conditions of the Pell-Lucas sequence $\{Q_n\}$ are $Q_0=1$ and $Q_1=1$. The primary instrument for identifying certain sequences is the Binet formula. The Binet's formulas for the Pell and Pell-Lucas numbers are

$$F_n=\frac{\Delta^n-\Theta^n}{\Delta-\Theta} \text{ and } L_n=\frac{\Delta^n+\Theta^n}{2} \tag{1.2}$$

respectively. Here, $\Delta=1+\sqrt{2}$ and $\Theta=1-\sqrt{2}$ are the roots of the equation $x^2-2x-1=0$.

Senturk and Unal (2022) developed this quaternion algebra and delineated its features. Let us represent its versors as $\{0,i_1,i_2,i_3\}$. Let τ_1,τ_2 and τ_3 be any nonzero real values. The versors adhere to the subsequent multiplication rules.

	i_1	i_2	i_3
i_1	$-\tau_1\tau_2$	$\tau_1 i_3$	$\tau_2 i_2$
i_2	$-\tau_1 i_3$	$-\tau_1\tau_3$	$\tau_3 i_1$
i_3	$\tau_2 i_2$	$-\tau_3 i_1$	$-\tau_2\tau_3$

Table1. Multiplication of the versors

Let K be the set of all 3-parameter generalized quaternions. Subsequently, we compose

$$\mathrm{K}=\{s_0+s_1i_1+s_2i_2+s_3i_3 : s_0,s_1,s_2,s_3\in\mathbb{R}\}.$$

Let $q=s_0+s_1i_1+s_2i_2+s_3i_3$ be a 3-parameter quaternion, then the conjugate of q, is $\bar{q}=s_0-s_1i_1-s_2i_2-s_3i_3$ and the norm of q is

$$N(q)=q\bar{q}=s_0^2+\tau_1\tau_2s_1^2+\tau_1\tau_3s_2^2+\tau_2\tau_3s_3^2.$$

Numerous studies exist about quaternions with coefficients obtained from Pell and Pell-Lucas numbers (Catarino, 2016; Cimen & Ipek, 2016; Aydin, Koklu & Yuce, 2017; Catarino & Vasco, 2017; Aydin, 2022; Catarino, 2018; Szynal-Liana & Wloch, 2016; Bilgici & Catarino, 2018; Brod, 2019; Aydin, 2018; Karatas & Halici, 2021)

In all studies, elements of integer sequences are arranged sequentially as quaternion coefficients. An alternative concept was initially developed by Daşdemir and Bilgici (2021). The quaternion coefficients were arranged randomly instead of sequentially. Subsequently, they broadened this concept to encompass all 2^N-ons (Bilgici and Dasdemir, 2020).

This concept has been employed by several authors concerning other hypercomplex numbers: Ait-Amrane and Tan (2024) investigated unrestricted dual-generalized complex Horadam numbers; Bhati and Kumar (2025) defined Fibonacci and Lucas octonions; Kizilaslan and Karabulut (2023) presented properties of unrestricted Tribonacci and Tribonacci-Lucas quaternions; Kizilates and Kone (2021) introduced higher-order hypercomplex numbers.

2. DEFINITIONS AND BINET FORMULAS

Let u_0, v_0 and z_0 be any integers. For any positive integer n, unrestricted Pell and Pell-Lucas 3-parameter generalized quaternions (UP3PGQ and UPL3PGQ) are defined as follows

$$A_n^{(u_1,u_2,u_3)} = P_n + \sum_{t=1}^{3} i_t P_{n+u_t} \tag{2.1}$$

and

$$B_n^{(u_1,u_2,u_3)} = Q_n + \sum_{t=1}^{3} i_t Q_{n+u_t} \tag{2.1}$$

respectively. These definitions with the recurrence relation (1.1) give

$$A_n^{(u,v,z)} = 2A_{n-1}^{(u,v,z)} + A_{n-2}^{(u,v,z)} \tag{2.3}$$

and

$$B_n^{(u,v,z)} = 2B_{n-1}^{(u,v,z)} + B_{n-2}^{(u,v,z)}. \tag{2.4}$$

Using the identities $P_{-n} = (-1)^{n+1}P_n$ and $Q_{-n} = (-1)^n Q_n$, we obtain

$$A_{-n}^{(u_1,u_2,u_3)} = (-1)^{n+1}\left[P_n + (-1)^{u_t}\sum_{t=1}^{3} i_t P_{n+u_t}\right]$$

and

$$B_{-n}^{(u_1,u_2,u_3)} = (-1)^{n}\left[Q_n + (-1)^{u_t}\sum_{t=1}^{3} i_t Q_{n+u_t}\right].$$

For UP3PGQ and UPL3PGQ, the following theorem contains the Binet's formulas.

Theorem 2.1. For any integer k, the kth UP3PGQ and UPL3PGQ are

$$A_k^{(u,v,z)} = \frac{\Delta^*\Delta^k - \Theta^*\Theta^k}{\Delta - \Theta} \text{ and } B_k^{(u,v,z)} = \frac{\Delta^*\Delta^k + \Theta^*\Theta^k}{2}$$

where $\Delta^* = 1 + i_1\Delta^u + i_2\Delta^v + i_3\Delta^z$ and $\Theta^* = 1 + i_1\Theta^u + i_2\Theta^z + i_3\Theta^z$.

Proof. Definition (2.1) and Binet formulas (1.2) gives

$$A_n^{(u,v,z)} = \frac{1}{\Delta - \Theta}[\Delta^n - \Theta^n + i_1(\Delta^{n+u} - \Theta^{n+u}) + i_2(\Delta^{n+v} - \Theta^{n+v}) + i_3(\Delta^{n+z} - \Theta^{n+z})]$$

$$= \frac{1}{\Delta - \Theta}[\Delta^n(1 + i_1\Delta^u + i_2\Delta^v + i_3\Delta^z) - \Theta^n(1 + i_1\Theta^u + i_2\Theta^v + i_3\Theta^z)].$$

The final equation validates the first Binet's formula within the theorem. The second can be acquired in a similar manner. ■

We require the subsequent lemma for later use.

Lemma 2.2. We have

$$\Delta^*\Theta^* = \Psi + \sqrt{2}\Omega \quad \text{and} \quad \Theta^*\Delta^* = \Psi - \sqrt{2}\Omega$$

where

$$\Psi = 2B_0^{(u,v,z)} - 1 - \tau_1\tau_2(-1)^u - \tau_1\tau_3(-1)^v - \tau_2\tau_3(-1)^z$$

and

$$\Omega = \mathrm{i}_1\tau_3(-1)^z P_{v-z} + i_2\tau_2(-1)^u P_{z-u} + i_3\tau_1(-1)^v P_{u-v}.$$

Proof. The proof is unequivocally straightforward by employing Binet's formulas (1.2) and Theorem 2.1. ■

Theorem 2.3 Generating functions for the sequences $\left\{A_k^{(u,v,z)}\right\}$ and $\left\{B_k^{(u,v,z)}\right\}$ are

$$\sum_{k=0}^{\infty} A_k^{(u,v,z)} q^k = \frac{A_0^{(u,v,z)} + q\left(A_1^{(u,v,z)} - 2A_0^{(u,v,z)}\right)}{1 - 2q - q^2}$$

and

$$\sum_{k=0}^{\infty} B_k^{(u,v,z)} q^k = \frac{B_0^{(u,v,z)} + q\left(B_1^{(u,v,z)} - 2B_0^{(u,v,z)}\right)}{1 - 2q - q^2}$$

respectively.

The proofs are clear and do not necessitate demonstration.

3. RESULTS

This section presents generalizations of several renowned identities. Let us begin with Vajda's identities.

Theorem 3.1. For any integers k, l and m, the followings hold

$$A_{k+l}^{(u,v,z)}A_{k+m}^{(u,v,z)} - A_{k}^{(u,v,z)}A_{k+l+m}^{(u,v,z)} = (-1)^k P_l[\Psi P_m - 2\Omega Q_m] \tag{3.1}$$

and

$$B_{k+l}^{(u,v,z)}B_{k+m}^{(u,v,z)} - B_{k}^{(u,v,z)}B_{k+l+m}^{(u,v,z)} = (-1)^{k+1} 2P_l[\Psi P_m - 2\Omega Q_m]. \tag{3.2}$$

Proof. Theorem 2.1 gives

$$\begin{aligned}
&A_{k+l}^{(u,v,z)}A_{k+m}^{(u,v,z)} - A_{k}^{(u,v,z)}A_{k+l+m}^{(u,v,z)} \\
&\quad = \frac{1}{(\Delta-\Theta)^2}[(\Delta^*\Delta^{k+l} - \Theta^*\Theta^{k+l})(\Delta^*\Delta^{k+m} - \Theta^*\Theta^{k+m}) \\
&\quad - (\Delta^*\Delta^{k} - \Theta^*\Theta^{k})(\Delta^*\Delta^{k+l+m} - \Theta^*\Theta^{k+l+m})] \\
&= \frac{1}{8}[-\Delta^*\Theta^*\Delta^{k+l}\Theta^{k+m} + \Delta^*\Theta^*\Delta^{k}\Theta^{k+l+m} - \Theta^*\Delta^*\Delta^{k+m}\Theta^{k+l} + \Theta^*\Delta^*\Delta^{k+l+m}\Theta^{k}] \\
&= \frac{(-1)^k}{8}[\Delta^*\Theta^*(-\Delta^l\Theta^m + \Theta^{l+m}) + \Theta^*\Delta^*(-\Delta^m\Theta^l + \Delta^{l+m})] \\
&= \frac{(-1)^k}{8}[\Delta^*\Theta^*\Theta^m(-\Delta^l + \Theta^l) + \Theta^*\Delta^*\Delta^m(-\Theta^l + \Delta^l)] \\
&= \frac{(-1)^k P_l}{2\sqrt{2}}[-\Delta^*\Theta^*\Theta^m + \Theta^*\Delta^*\Delta^m] \\
&= \frac{(-1)^k P_l}{2\sqrt{2}}\left[-\left(\Psi + 2\sqrt{2}\Omega\right)\Theta^m + \left(\Psi - 2\sqrt{2}\Omega\right)\Delta^m\right] \\
&= \frac{(-1)^k P_l}{2\sqrt{2}}\left[\Psi(\Delta^m - \Theta^m) - 2\sqrt{2}\Omega(\Delta^m + \Theta^m)\right].
\end{aligned}$$

The final equation proves Eq. (3.1). Again Theorem 2.1 gives

$$\begin{aligned}
&B_{k+l}^{(u,v,z)}B_{k+m}^{(u,v,z)} - B_{k}^{(u,v,z)}B_{k+l+m}^{(u,v,z)} \\
&\quad = (\Delta^*\Delta^{k+l} + \Theta^*\Theta^{k+l})(\Delta^*\Delta^{k+m} + \Theta^*\Theta^{k+m}) \\
&\quad - (\Delta^*\Delta^{k} + \Theta^*\Theta^{k})(\Delta^*\Delta^{k+l+m} + \Theta^*\Theta^{k+l+m}) \\
&= \Delta^*\Theta^*\Delta^{k+l}\Theta^{k+m} - \Delta^*\Theta^*\Delta^{k}\Theta^{k+l+m} + \Theta^*\Delta^*\Delta^{k+m}\Theta^{k+l} - \Theta^*\Delta^*\Delta^{k+l+m}\Theta^{k} \\
&= (-1)^{k+1}[\Delta^*\Theta^*(-\Delta^l\Theta^m + \Theta^{l+m}) + \Theta^*\Delta^*(-\Delta^m\Theta^l + \Delta^{l+m})] \\
&= (-1)^{k+1}[\Delta^*\Theta^*\Theta^m(-\Delta^l + \Theta^l) + \Theta^*\Delta^*\Delta^m(-\Theta^l + \Delta^l)]
\end{aligned}$$

$$= (-1)^{k+1}2\sqrt{2}\,P_l[-\Delta^*\Theta^*\Theta^m + \Theta^*\Delta^*\Delta^m]$$

$$= (-1)^{k+1}2\sqrt{2}\,P_l\left[-\left(\Psi + 2\sqrt{2}\Omega\right)\Theta^m + \left(\Psi - 2\sqrt{2}\Omega\right)\Delta^m\right]$$

$$= (-1)^{k+1}2\sqrt{2}\,P_l\left[\Psi(\Delta^m - \Theta^m) - 2\sqrt{2}\Omega(\Delta^m + \Theta^m)\right].$$

The last equation proves Eq. (3.1). ■

The Catalan's identities presented in the subsequent theorem can be derived from Vajda's identities by substituting m with $-l$.

Theorem 3.2. For any integers k and l, the followings hold

$$A_{k+l}^{(u,v,z)}A_{k-l}^{(u,v,z)} - \left[A_k^{(u,v,z)}\right]^2 = (-1)^{k+l+1}[\Psi P_l^2 + \Omega P_{2l}] \tag{3.3}$$

and

$$B_{k+l}^{(u,v,z)}B_{k-l}^{(u,v,z)} - \left[B_k^{(u,v,z)}\right]^2 = (-1)^{k+l}2[\Psi P_l^2 + \Omega P_{2l}]. \tag{3.4}$$

The proof of Theorem 3.2 requires the identity $P_{2r} = 2P_rQ_r$. The Cassini's identities outlined in the following theorem can be obtained from Theorem 3.2 by substituting l with 1.

Theorem 3.3. For any integer k, the followings hold

$$A_{k+1}^{(u,v,z)}A_{k-1}^{(u,v,z)} - \left[A_k^{(u,v,z)}\right]^2 = (-1)^k[\Psi + 2\Omega] \tag{3.5}$$

and

$$B_{k+1}^{(u,v,z)}B_{k-1}^{(u,v,z)} - \left[B_k^{(u,v,z)}\right]^2 = (-1)^{k+1}2[\Psi + 2\Omega]. \tag{3.6}$$

A notable identity is d'Ocagne's identity presented in the subsequent theorem can be derived from Vajda's identities by substituting l with 1 and m with $r - k$

Theorem 3.4. For any integers k and r, the followings hold

$$A_{k+1}^{(u,v,z)}A_r^{(u,v,z)} - A_k^{(u,v,z)}A_{r+1}^{(u,v,z)} = (-1)^{k+1}[-\Psi P_{r-k} + 2\Omega Q_{r-k}\,] \tag{3.7}$$

and

$$B_{k+1}^{(u,v,z)}B_r^{(u,v,z)} - B_k^{(u,v,z)}B_{r+1}^{(u,v,z)} = (-1)^k2[-\Psi P_{r-k} + 2\Omega Q_{r-k}\,]. \tag{3.8}$$

The subsequent identities can be demonstrated with definitions, recurrence relations, and Binet formulas for the UP3PG and UPL3PG quaternions.

Theorem 3.5. For any integers k and l, we have

$$B_k^{(u,v,z)} + B_{k-1}^{(u,v,z)} = 2A_k^{(u,v,z)},$$

$$A_k^{(u,v,z)} + A_{k-1}^{(u,v,z)} = B_k^{(u,v,z)},$$

$$A_{k+1}^{(u,v,z)} + A_{k-1}^{(u,v,z)} = 2B_k^{(u,v,z)},$$

$$A_k^{(u,v,z)} + B_k^{(u,v,z)} = A_{k+1}^{(u,v,z)},$$

$$B_{k+1}^{(u,v,z)} + B_{k-1}^{(u,v,z)} = 4A_k^{(u,v,z)},$$

$$A_{k+l}^{(u,v,z)} + (-1)^l A_{k+l}^{(u,v,z)} = 2Q_l A_k^{(u,v,z)},$$

$$B_{k+l}^{(u,v,z)} + (-1)^l B_{k+l}^{(u,v,z)} = 2Q_l B_k^{(u,v,z)},$$

$$A_k^{(u,v,z)} + A_{k+1}^{(u,v,z)} + A_{k+3}^{(u,v,z)} = 2A_{k+2}^{(u,v,z)},$$

$$B_k^{(u,v,z)} + B_{k+1}^{(u,v,z)} + B_{k+3}^{(u,v,z)} = 3B_{k+2}^{(u,v,z)}.$$

REFERENCES

Ait-Amrane, N. R., & Tan, E. (2024). On unrestricted dual-generalized complex Horadam numbers. *Communications Faculty of Sciences University of Ankara Series A1 Mathematics and Statistics*, 73(2), 517-528.

Aydin, F. T. (2018). On bicomplex Pell and Pell-Lucas numbers. *Communications in Advanced Mathematical Sciences, 1*(2), 142-155.

Aydin, F. T. (2022). Dual-hyperbolic Pell quaternions. *Journal of Discrete Mathematical Sciences and Cryptography, 25*(5), 1321-1334.

Aydin, F. T., Koklu, K., & Yuce, S. (2017). Generalized dual Pell quaternions. *Notes on Number Theory and Discrete Mathematics, 23*(4), 66-84.

Bhati, J., & Kumar, S. D. (2025). Unrestricted Fibonacci and Lucas octonions. *Palestine Journal of Mathematics*, 14(2).

Bilgici, G., & Catarino, P. (2018). Unrestricted Pell and Pell-Lucas quaternions. *International Journal of Mathematics and Systems Science*, 1(3), 1-4.

Bilgici, G., & Daşdemir, A. (2020). Some unrestricted Fibonacci and Lucas hyper-complex numbers. *Acta et Commentationes Universitatis Tartuensis de Mathematica*, 24(1), 37-48.

Brod, D. (2019). On a new generalization of split Pell quaternions. *Mathematica Applicanda, 47*(2), 245-258.

Catarino, P. (2016). The modified Pell and the modified k-Pell quaternions and octonions. *Advances in Applied Clifford Algebras, 26*, 577-590.

Catarino, P. (2018). On hyperbolic k-Pell quaternions sequences. *Annales Mathematicae et Informaticae*, 49, 61-73.

Catarino, P., & Vasco, P. (2017). On dual k-Pell quaternions and octonions. *Mediterranean Journal of Mathematics, 14*(2), 75.

Cimen, C. B., & Ipek, A. (2016). On Pell quaternions and Pell-Lucas quaternions. *Advances in Applied Clifford Algebras, 26*, 39-51.

Daşdemir, A., & Bilgici, G. (2021). Unrestricted Fibonacci and Lucas quaternions. *Fundamental Journal of Mathematics and Applications*, 4(1), 1-9.

Karatas, A., & Halici, S. (2021). Some properties of bicomplex Pell and Pell-Lucas numbers. *Journal of Information and Optimization Sciences, 42*(3), 701-709.

Kızılaslan, G., & Karabulut, L. (2023). Unrestricted Tribonacci and Tribonacci–Lucas quaternions, *Notes on Number Theory and Discrete Mathematics*, 29(2), 310-321.

Kızılateş, C., & Kone, T. (2021). On higher order Fibonacci hyper complex numbers. *Chaos, Solitons & Fractals*, 148, 111044.

Koshy, T. (2014). *Pell and Pell-Lucas numbers with applications*. New York: Springer.

Senturk, T. D., & Unal, Z. (2022). 3-parameter generalized quaternions. *Computational Methods and Function Theory*, 22(3), 575-608.

Szynal-Liana, A., & Wloch, I. (2016). The Pell quaternions and the Pell octonions. *Advances in Applied Clifford Algebras, 26*, 435-440.

Chapter 4

A DIFFERENT APPROACH TO DISCONTINUOUS BEAM ANALYSIS

B. Gültekin SINIR[1], Duygu DÖNMEZ DEMİR[2],

Emine KAHRAMAN[3]

1 Prof. Dr., Manisa Celal Bayar University, Faculty of Engineering and Natural Sciences, Civil Engineering, Manisa, gultekin.sinir@cbu.edu.tr, ORCID: orcid.org/0000-0002-9478-1666
2 Prof. Dr., Manisa Celal Bayar University, Faculty of Engineering and Natural Sciences, Department of Mathematics, Manisa, duygu.donmez@cbu.edu.tr, ORCID: orcid.org/0000-0003-0886-624X
3 Ph.D. Student, Manisa Celal Bayar University, Graduate School of Education, emine.35@hotmail.com, ORCID: orcid.org/0000-0002-6876-6817

Introduction

Discontinuous beams are statically determinate systems that lack moment continuity between spans, with each span carrying the load independently. Such systems are widely preferred, particularly in prefabricated construction applications, due to their easy of assembly, standardized production, and tolerance to temperature fluctuations and shrinkage. However, the lack of moment transfer results in larger deflections and cross-sectional moments compared to continuous systems. Therefore, accurately modeling the behavior of discontinuous beams is a critical engineering requirement for ensuring safe and economical design.

The stability and vibration behavior of elastic beams have been extensively investigated in the classical literature (Timoshenko & Gere, 1961; Paidoussis, 1998). Subsequent studies have shown that by adding intermediate elastic supports to beams, critical speeds and natural frequencies change, allowing structures to operate safely at higher speeds. *(Wang, Friswell & Lei, 2006; Behdinan & Tabarrok, 1997).* Recently, the analysis of elastically supported beams has become more systematic thanks to the modeling of discontinuities with Dirac delta or Heaviside functions. *(Dönmez Demir, Sınır & Kahraman, 2019).* In addition, in the study of Zhu et al. *(2025)*, a closed form solution was obtained in fluid-carrying pipes, clearly demonstrating the contribution of elastic supports to system stability.

This study investigates the dynamic behavior of beams supported by linear elastic springs. The discontinuity of the structure is modeled by locating the springs at specific points, thus expressing them using differential equations that include discontinuity functions, unlike classical continuous systems. In the considered system, the stiffness coefficients and locations of the elastic springs significantly affect the critical speed values and vibration modes of the system.

In this study, the solution to the beam's equation of motion was easily obtained using analytical techniques thanks to a special assumption. This assumption eliminated the difficulties encountered in solving a nonhomogeneous equation involving a discontinuity function. The generated solutions were evaluated for different boundary conditions and spring placement scenarios, and the critical speeds of the system were calculated.

Solution of Mathematical Model

In this section, we will consider a beam supported by linear elastic springs. Then, the equation of motion (*Zhu et. al., 2025*) involving a discontinuous function with elastic springs, n is introduced as

$$y^{iv} + \lambda^2 y'' + \sum_{i=1}^{n} k_i y(x_i)\delta(x - x_i) = 0 \tag{1}$$

where λ represents the critical velocity value, k_i, δ is the spring coefficient and Dirac delta function, respectively. $y(x)$ represents the transverse displacement. The derivatives denote differentiation with respect to spatial variable. In the Eq. (1), let's assume that

$$Q(x) = \sum_{i=1}^{n} k_i y(x_i)\delta(x - x_i) \tag{2}$$

Then, the resulting equation is obtained as

$$y^{iv} + \lambda^2 y'' = -Q(x) \tag{3}$$

Thus, the equation of motion including the discontinuity function becomes a fourth-order, linear nonhomogeneous differential equation that can be solved. Then, the solution of homogeneous part of the Eq. (3) is found as

$$y_h = c_1 + c_2 x + c_3 \cos \lambda x + c_4 \sin \lambda x \tag{4}$$

The variation of parameters method can be used to solve equations involving special functions such as the Heaviside and Dirac delta functions. The particular solution using this method is obtained by assuming the constant coefficients c_1, c_2, c_3 and c_4 in Eq. (4) to depend on x and the following equation is obtained

$$y_p = c_1(x) + c_2(x)x + c_3(x) \cos \lambda x + c_4(x) \sin \lambda x \tag{5}$$

If the Eq. (5) are differentiated and the necessary assumptions are performed, the following matrix equation is obtained;

$$\begin{bmatrix} 1 & x & cos(\lambda x) & sin(\lambda x) \\ 0 & 1 & -\lambda \sin(\lambda x) & \lambda cos(\lambda x) \\ 0 & 0 & \lambda^2 cos(\lambda x) & \lambda^2 sin(\lambda x) \\ 0 & 0 & \lambda^3 sin(\lambda x) & \lambda^3 cos(\lambda x) \end{bmatrix} \begin{bmatrix} c_1' \\ c_2' \\ c_3' \\ c_4' \end{bmatrix} = \begin{bmatrix} 0 \\ 0 \\ 0 \\ Q(x) \end{bmatrix} \tag{6}$$

The solution of system (6) yields

$$c_1'(x) = \frac{Q(x)x}{\lambda^2} \tag{7}$$

$$c_2'(x) = -\frac{Q(x)}{\lambda^2} \tag{8}$$

$$c_3'(x) = -\frac{Q(x) \sin(\lambda x)}{\lambda^3} \tag{9}$$

$$c_4'(x) = \frac{Q(x) \cos(\lambda x)}{\lambda^3} \tag{10}$$

Substituting Eq. (2) into the above equations and integrating the resulting equations give

$$c_1(x) = \sum_{i=1}^{n} \frac{k}{\lambda^2} x\, y(x)\, H(x - x_i) + c_1 \tag{11}$$

$$c_2(x) = -\sum_{i=1}^{n} \frac{k}{\lambda^2} y(x)\, H(x - x_i) + c_2 \tag{12}$$

$$c_3(x) = -\sum_{i=1}^{n} \frac{k}{\lambda^3} y(x)\, H(x - x_i) \sin(\lambda x) + c_3 \tag{13}$$

$$c_4(x) = \sum_{i=1}^{n} \frac{k}{\lambda^3} y(x)\, H(x - x_i) \cos(\lambda x) + c_4 \tag{14}$$

where $H(x - x_i)$ is Heaviside function. Then, the solution to the equation of motion is obtained as

$$y(x) = c_1 + c_2 x + c_3\, cos(\lambda x) + c_4\, sin(\lambda x) + \sum_{i=1}^{n} \frac{k_i}{\lambda^2} y(x_i) H(x - x_i) \left[-(x - x_i) + \frac{sin\, \lambda(x - x_i)}{\lambda} \right] \tag{15}$$

Writting the general solution (15) for $y(x_i)$ and considering the properties of the Heaviside function yield

$$y(x_i) = c_1 + c_2 x_i + c_3\, cos(\lambda x_i) + c_4\, sin(\lambda x_i) + \sum_{j=1}^{n} \frac{k_j}{\lambda^2} y(x_j) \left[-(x_i - x_j) + \frac{sin\, \lambda(x_i - x_j)}{\lambda} \right] \tag{16}$$

If Eq. (16) is rearranged for $y(x_j)$, the following equation is found;

$$y(x_i) = c_1 + c_2 x_i + c_3\, cos(\lambda x_i) + c_4\, sin(\lambda x_i) + \sum_{j=1}^{n} \frac{k_j}{\lambda^2} \left[-(x_i - x_j) + \frac{sin\, \lambda(x_i - x_j)}{\lambda} \right] \times \left\{ \begin{matrix} c_1 + c_2 x_j + c_3\, cos(\lambda x_j) + c_4\, sin(\lambda x_j) \\ + \sum_{l=1}^{n} \frac{k_j}{\lambda^2} y(x_l) \left[-(x_j - x_l) + \frac{sin\, \lambda(x_j - x_l)}{\lambda} \right] \end{matrix} \right\} \tag{17}$$

Performing the necessary mathematical processes, the general solution for a beam containing springs, n is obtained as

$$\begin{aligned} y(x) = c_1 & \left\{ 1 + \sum_{i=1}^{n} \frac{k_i}{\lambda^2} \mu_{1i} \left[-(x - x_i) + \frac{sin\, \lambda(x - x_i)}{\lambda} \right] H(x - x_i) \right\} \\ + c_2 & \left\{ x + \sum_{i=1}^{n} \frac{k_i}{\lambda^2} \mu_{2i} \left[-(x - x_i) + \frac{sin\, \lambda(x - x_i)}{\lambda} \right] H(x - x_i) \right\} \\ + c_3 & \left\{ cos(\lambda x) + \sum_{i=1}^{n} \frac{k_i}{\lambda^2} \mu_{1i} \left[-(x - x_i) + \frac{sin\, \lambda(x - x_i)}{\lambda} \right] H(x - x_i) \right\} \\ + c_4 & \left\{ sin(\lambda x) + \sum_{i=1}^{n} \frac{k_i}{\lambda^2} \mu_{1i} \left[-(x - x_i) + \frac{sin\, \lambda(x - x_i)}{\lambda} \right] H(x - x_i) \right\} \end{aligned} \tag{18}$$

where

$$\mu_{11} = 1,$$

$$\mu_{1i} = 1 + \sum_{j=1}^{n} \frac{k_j}{\lambda^2}\left[-(x_i - x_j) + \frac{sin\,\lambda(x_i - x_j)}{\lambda}\right]\mu_{1j},$$

$$\mu_{21} = x_i,$$

$$\mu_{2i} = x_i + \sum_{j=1}^{n} \frac{k_j}{\lambda^2}\left[-(x_i - x_j) + \frac{sin\,\lambda(x_i - x_j)}{\lambda}\right]\mu_{2j},$$

$$\mu_{31} = cos(\lambda x_i),$$

$$\mu_{3i} = cos(\lambda x_i) + \sum_{j=1}^{n} \frac{k_j}{\lambda^2}\left[-(x_i - x_j) + \frac{sin\,\lambda(x_i - x_j)}{\lambda}\right]\mu_{3j},$$

$$\mu_{41} = sin(\lambda x_i),$$

$$\mu_{4i} = sin(\lambda x_i) + \sum_{j=1}^{n} \frac{k_j}{\lambda^2}\left[-(x_i - x_j) + \frac{sin\,\lambda(x_i - x_j)}{\lambda}\right]\mu_{4j},$$

$$i \geq 2. \tag{19}$$

Applications

1. Analysis of Dynamic Behavior of Simply-Simply Supported Single-Span Elastic Beam

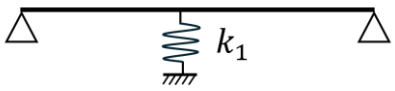

Figure 1. Two-span elastic beam

The dynamic behavior of a two-span elastic beam under simply-simply supported condition

$$y(0) = 0, \qquad y''(0) = 0, \qquad y(1) = 0, \qquad y''(1) = 0 \tag{20}$$

is obtained as

$$y(x) = c_1\left(1 + \frac{k_1}{\lambda^2}H(x - x_1)\left[\frac{\sin\lambda\,(x - x_1)}{\lambda} - (x - x_1)\right]\right)$$
$$+c_2\left(x + \frac{k_1}{\lambda^2}x_1 H(x - x_1)\left[\frac{\sin\lambda\,(x - x_1)}{\lambda} - (x - x_1)\right]\right)$$
$$+c_3\left(\cos(\lambda x) + \frac{k_1}{\lambda^2}\cos(\lambda x_1)\,H(x - x_1)\left[\frac{\sin\lambda\,(x - x_1)}{\lambda} - (x - x_1)\right]\right)$$
$$+c_4\left(\sin(\lambda x) + \frac{k_1}{\lambda^2}sin(\lambda x_1)\,H(x - x_1)\left[\frac{\sin\lambda\,(x - x_1)}{\lambda} - (x - x_1)\right]\right) \tag{21}$$

The Table 1 shows the comparison of the critical speed values λ obtained from the classical solution (Sınır & Sınır, 2011) with those found by the present method (bold) for different stiffness values k_1 and spring position x_1.

Table 1. Comparison of critical speed values, λ for different values, k_1

x_1	$k_1 = 100$	$\boldsymbol{k_1 = 100}$	$k_1 = 1000$	$\boldsymbol{k_1 = 1000}$
0.1	11.6355	**11.6355**	18.6836	**18.6836**
0.3	20.4587	**20.4587**	30.7234	**30.7234**
0.5	29.2960	**29.2960**	39.4784	**39.4784**

Considering the numerical results obtained, it is seen that the solutions obtained with the current method are consistent when compared with the classical solution.

2. Dynamic Analysis of Simply-Simply Supported Three-Span Elastic Beam

In this section, the dynamic behavior of a simple-simply supported three-span elastic beam will be analyzed. If the general solution is arranged for n = 2,

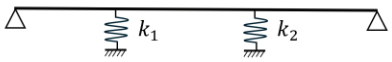

Figure 2. Three-span elastic beam

$$
\begin{aligned}
y(x) \;=\; c_1 & \left(\begin{array}{l} 1+\frac{k_1}{\lambda^2}H(x-x_1)\left[-(x-x_1)+\frac{\sin\lambda(x-x_1)}{\lambda}\right] \\ +\frac{k_2}{\lambda^2}H(x-x_2)\left[-(x-x_2)+\frac{\sin\lambda(x-x_2)}{\lambda}\right] \\ \times\left[1\pm\frac{k_1}{\lambda^2}\left((x_2-x_1)+\frac{\sin\lambda(x_2-x_1)}{\lambda}\right)\right] \end{array} \right) \\
+c_2 & \left(\begin{array}{l} x+\frac{k_1}{\lambda^2}x_1H(x-x_1)\left[-(x-x_1)+\frac{\sin\lambda(x-x_1)}{\lambda}\right] \\ +\frac{k_2}{\lambda^2}H(x-x_2)\left[-(x-x_2)+\frac{\sin\lambda(x-x_2)}{\lambda}\right] \\ \times\left[x_2\pm\frac{k_1}{\lambda^2}x_1\left((x_2-x_1)+\frac{\sin\lambda(x_2-x_1)}{\lambda}\right)\right] \end{array} \right) \\
+c_3 & \left(\begin{array}{l} \cos(\lambda x)+\frac{k_1}{\lambda^2}\cos(\lambda x_1)\,H(x-x_1)\left[-(x-x_1)+\frac{\sin\lambda(x-x_1)}{\lambda}\right] \\ +\frac{k_2}{\lambda^2}H(x-x_2)\left[-(x-x_2)+\frac{\sin\lambda(x-x_2)}{\lambda}\right] \\ \times\left[\cos(\lambda x_2)\pm\frac{k_1}{\lambda^2}\cos(\lambda x_1)\left((x_2-x_1)+\frac{\sin\lambda(x_2-x_1)}{\lambda}\right)\right] \end{array} \right) \\
+c_4 & \left(\begin{array}{l} \sin(\lambda x)+\frac{k_1}{\lambda^2}\sin(\lambda x_1)\,H(x-x_1)\left[-(x-x_1)+\frac{\sin\lambda(x-x_1)}{\lambda}\right] \\ +\frac{k_2}{\lambda^2}H(x-x_2)\left[-(x-x_2)+\frac{\sin\lambda(x-x_2)}{\lambda}\right] \\ \times\left[\sin(\lambda x_2)\pm\frac{k_1}{\lambda^2}\sin(\lambda x_1)\left((x_2-x_1)+\frac{\sin\lambda(x_2-x_1)}{\lambda}\right)\right] \end{array} \right) \qquad (22)
\end{aligned}
$$

The simple-simple support boundary conditions (20) are applied to the general solution and critical speed values are calculated for different stiffness values and spring positions.

Table 2. The critical speed values, λ obtained from the method for different stiffness values, k_1, k_2 and spring position values, x_1, x_2

x_1	x_2	$k_1 = 100$ $k_2 = 0$	$k_1 = 1000$ $k_2 = 0$	$k_1 = 100$ $k_2 = 100$	$k_1 = 1000$ $k_2 = 1000$
0.1	0.6	11.6355	18.6836	28.7510	54.0755
0.3	0.6	20.4587	30.7234	40.2442	73.2774
0.5	0.6	29.2960	39.4784	35.5453	46.3596

Table 2 shows that the critical speed increases significantly as the stiffness values, k_1 and k_2 increase. This raise confirms that the resonance frequency increases with increasing system stiffness. The presence of two springs ($k_1 \neq 0, k_2 \neq 0$) significantly increases the stiffness of the system, and when both k_1 and k_2 are present, the critical speed rises even more compared to the single spring case. This indicates that the system becomes more stable against vibration. As x_1 grows, the critical speed also increases, and the spring's position towards the center of the span increases its contribution to stiffness, increasing the system's resonance speed. When these values fall below operating speeds in

machines, shafts, or beam systems, there is a risk of resonance. Therefore, increasing the critical speed allows the design to transition to the safety zone.

Conclusion

The dynamic behavior of both single-spring and multiple-spring beam systems, depending on the stiffness coefficient and location parameters, is compared using application examples. The compatibility of the results with classical methods demonstrates the validity of the approach and demonstrates its potential to contribute to engineering applications.

The critical speed tends to increase as the system stiffness increases. As the elastic spring stiffness increases, the system becomes more rigid, thus increasing natural frequencies and critical speeds. This is desirable in shaft and beam systems operating in vibrating environments because it removes the system from the resonant region. The spring's position influences the mode shapes. A spring positioned in the center of the span, in particular, affects symmetric modes more strongly. Springs placed near the edge may be less effective than those in lower modes, but they can significantly alter the critical speeds of the upper modes. It is observed that critical speeds increase when springs are added. This indicates that the system's stiffness increases, allowing it to operate safely at higher speeds. In real-world engineering applications such as rotating machinery, shaft systems, and conveyors, critical speeds must be above operating speeds. If the values in the table are too close to operating speeds, the system may resonate and cause damage. Therefore, spring stiffness and placement should be selected to ensure that critical speeds exceed the desired limits.

As a result, critical speeds are seen to be extremely important in engineering design, reflecting the vibration behavior of the system, depending on both its stiffness and boundary conditions, for both strength and vibration safety. The results obtained from the tables will contribute to design optimization, ensuring that the system operates outside of resonance.

Acknowledgement

Emine Kahraman is supported by TÜBİTAK under the TÜBİTAK Science Fellowships and Grant Programme Directorate (BİDEB) 2211-National PhD Scholarship Programs.

References

Abrate, S. (1995). Vibration of nonuniform and discontinuous beams. *Journal of Sound and Vibration, 185*(4), 703–716.

Behdinan, K., & Tabarrok, B. (1997). Vibration and stability of beams with elastic supports. *Journal of Sound and Vibration, 204*(1), 43–61.

Blevins, R. D. (2015). *Formulas for natural frequency and mode shape*. John Wiley & Sons.

Dönmez Demir, D., Sınır, B. G., & Kahraman, E. (2019). The solution of the governing equation of the beam on linear spring foundation modeled by a discontinuity function. *Sigma Journal of Engineering and Natural Sciences, 37*(2), 495–506.

Dönmez Demir, D., Sınır, B. G., & Kahraman, E. (2021). Dynamical analysis of the general beam model with singularity function. *Journal of Engineering Research, 9*(3), 52-63.

Huang, M. H., & Hsu, Y. C. (2005). Dynamic analysis of beams with multiple elastic supports. *Computers & Structures, 83*(21–22), 1736–1750.

Kahraman, E., Dönmez Demir, D., & Sınır, B. G. (2018). Pertürbasyon-sonlu farklar metodunun titreşim problemlerine uygulanması. *Manisa Celal Bayar Üniversitesi, Fen Bilimleri Enstitüsü*.

Mao, Q. (2012). Free vibration analysis of elastically connected multiple-beams by using the Adomian modified decomposition method. *Journal of Sound and Vibration, 331*(11), 2532–2542.

Nayfeh, A. H., & Emam, S. A. (2008). Exact solution and stability of postbuckling configurations of beams. *Nonlinear Dynamics, 54*, 395–408.

Paidoussis, M. P. (1998). *Fluid-structure interactions: Slender structures and axial flow*. Academic Press.

Paidoussis, M. P., Price, S. J., & de Langre, E. (2010). *Fluid-structure interactions: Cross-flow-induced instabilities*. Cambridge University Press.

Rao, S. S. (2007). *Vibration of continuous systems*. John Wiley & Sons.

Sınır, B. G. (2013). Pseudo-nonlinear dynamic analysis of buckled pipes. *Journal of Fluids and Structures, 37*, 151–170.

Sınır, B. G., & Sınır, S. (2011). Eksenel parametrik zorlamalı çok yaylı kirişlerin yeni bir yaklaşımla dinamik analizi. *XVII. Ulusal Mekanik Kongresi*, Fırat Üniversitesi, Elazığ, Türkiye.

Thorsen, M. J., Challabotla, N. R., Sævik, S., & Nydal, O. J. (2019). A numerical study on vortex-induced vibrations and the effect of slurry density variations on fatigue of ocean mining risers. *Ocean Engineering, 174*, 1–13.

Wang, D., Friswell, M. I., & Lei, Y. (2006). Maximizing the natural frequency of a beam with an intermediate elastic support. *Journal of Sound and Vibration, 291*(3–5), 1229–1238.

Yulin, F., Lizhong, J., & Wangbao, Z. (2020). Dynamic response of a three-beam system with intermediate elastic connections under a moving load/mass-spring. *Earthquake Engineering and Engineering Vibration, 19*(2), 377–395.

Zhu, B., Feng, J. Z., Guo, Y., & Wang, Y. Q. (2025). Exact closed-form solution for buckling and free vibration of pipes conveying fluid with intermediate elastic supports. *Journal of Sound and Vibration, 596*, 118762.

Chapter 5

A NEW CONTRACTION ON PARTIAL METRIC SPACES

Mustafa ASLANTAŞ[1]

1 Doç. Dr., Çankırı Karatekin University, Faculty of Science, Department of Mathematics,

Orcid: 0000-0003-4338-3518

1-INTRODUCTION

Fixed point theory is a key topic of nonlinear analysis that has been widely applied in various branches of mathematics, including optimization theory, dynamical systems, differential equations and mathematical economics. Since the pioneering Banach contraction principle [2], A wide number of contractive criteria have been developed and tested to assure the existence and uniqueness of fixed points in metric and generalized metric spaces.These innovations have considerably enhanced the subject's theoretical foundation and broadened its applicability to more complicated and abstract settings [7, 14, 16, 17].

Many practical and theoretical problems, however, do not ensure the presence of a fixed point, especially when the underlying mapping is established between two independent subsets of a metric space rather than from a set into itself. This limitation has driven the development of best proximity point theory, which may be thought of as a natural extension of fixed point theory [4]. The primary goal of this theory is to find an element whose image under the provided mapping is as close to itself as possible, meaning that the gap between the point and its image is as little as possible, namely the distance between the involved sets. Best proximity point theory has been successfully developed for various classes of mappings and spaces, providing powerful tools for addressing non-self mappings in metric and normed spaces [1, 3, 5, 8, 9, 10, 19].

In contrast, classical contraction criteria frequently impose stringent assumptions that ensure the fixed or best proximity point's uniqueness. Nonetheless, many mappings in real-world applications do not meet such stringent requirements and may permit several fixed points or optimal proximity points. This observation has sparked increased interest in non-unique contraction maps, which lower classical contractive constraints while ensuring the presence of solutions. Such mappings have been investigated using a variety of frameworks, including multivalued mappings, generalized contractions, and weak contractive conditions, revealing rich structural characteristics and wide applicability. The link between best proximity point theory and non-unique contraction conditions has been the subject of much discussion in recent years. Researchers have concentrated on developing existence results, convergence theorems, and stability properties for the optimal proximity points while avoiding uniqueness assumptions. These studies not only generalize some well-known fixed point results, but also provide more information about the behavior of non-self mappings under weaker contractive circumstances [6, 11, 12, 15].

Motivated by these findings, the current research seeks to investigate the optimum proximity point outcomes for a class of non-unique contraction mappings in metric space. By adding proper contractive conditions and applying appropriate geometric and topological tools, we obtain new existence theorems that expand and unify various existing results in the literature. Illustrative examples are presented to demonstrate the efficacy of the proposed method and emphasize the benefits of the achieved results.

2-PRELIMINARIES

Matthews [13] obtained additional generalization of the Banach's fundamental result by introducing a well-known the following notion. We will now review the notion of a partial metric space and some of its fundamental features.

Definition 1

Let $\Gamma: 6 \times 6 \to [0, \infty)$ be a function satisfying the following, every point $p, d, z \in 6$,

P1) $\Gamma(\mathfrak{p},\mathfrak{p}) = \Gamma(\mathfrak{p},\mathfrak{d}) = \Gamma(\mathfrak{d},\mathfrak{d})$ if and only if $\mathfrak{p} = \mathfrak{d}$

P2) $\Gamma(\mathfrak{p},\mathfrak{p}) \leq \Gamma(\mathfrak{p},\mathfrak{d})$,

P3) $\Gamma(\mathfrak{p},\mathfrak{d}) = \Gamma(\mathfrak{d},\mathfrak{p})$,

P4) $\Gamma(\mathfrak{p},\mathfrak{d}) \leq \Gamma(\mathfrak{p},z) + \Gamma(z,\mathfrak{d}) - \Gamma(z,z)$

Then $(\mathcal{G},\Gamma)$ is called a partial metric space (shortly prtl. m. s.).

While any metric space can be regarded as a special case of a prtl. m. s., the reverse implication fails in general. In fact, let $\mathcal{G} = [0,\infty)$ and let $\Gamma: \mathcal{G}\times\mathcal{G} \to [0,\infty)$ be defined by

$$\Gamma(\mathfrak{p},\mathfrak{d}) = \max\{\mathfrak{p},\mathfrak{d}\}$$

for all $\mathfrak{p},\mathfrak{d} \in \mathcal{G}$. While $(\mathcal{G},\Gamma)$ is a prtl m. s., it cannot be regarded as a metric space.

The sets

$$B_\Gamma(\mathfrak{p},\varepsilon) = \{\mathfrak{d} \in \mathcal{G}: \Gamma(\mathfrak{p},\mathfrak{d}) < \Gamma(\mathfrak{p},\mathfrak{p}) + \varepsilon\},$$

for all $\mathfrak{p} \in \mathcal{G}$ and $\varepsilon > 0$ where $(\mathcal{G},\Gamma)$ is a prtl. m. s., are called open balls. Let $\mathfrak{p} \in \mathcal{G}$ and let $\{\mathfrak{p}_n\}$ be a sequence in $\mathcal{G}$. Then, $\{\mathfrak{p}_n\}$ converges to $\mathfrak{p}$ with respect to τ_Γ if and only if

$$\lim_{r\to\infty} \Gamma(\mathfrak{p}_r,\mathfrak{p}) = \Gamma(\mathfrak{p},\mathfrak{p}).$$

If the limit

$$\lim_{n,m\to\infty} \Gamma(\mathfrak{p}_n,\mathfrak{p}_m) = L$$

where $L \in \mathbb{R}$, then the sequence $\{\mathfrak{p}_n\}$ is called a Cauchy. Moreover, $(\mathcal{G},\Gamma)$ is said to be complete if each Cauchy $\{\mathfrak{p}_n\}$ in $\mathcal{G}$ is convergent to some point $\mathfrak{p} \in \mathcal{G}$ such that

$$\Gamma(\mathfrak{p},\mathfrak{p}) = \lim_{n,m\to\infty} \Gamma(\mathfrak{p}_n,\mathfrak{p}_m).$$

A weaker completeness condition in prtl. m. s.s, known as 0-completeness, was introduced by Romaguera [18] in recent years.

Definition 2
Let $\{\mathfrak{p}_n\}$ be a sequence in a prtl. m. s.$(\mathcal{G},\Gamma)$.

(i) The sequence $\{\mathfrak{p}\}$ is said to be 0-Cauchy if

$$\lim_{n,m\to\infty} \Gamma(\mathfrak{p}_n,\mathfrak{p}_m) = 0.$$

(ii) The space $(\mathcal{G},\Gamma)$ is said to be 0-complete if each 0-Cauchy is convergent to a point $\xi \in \mathcal{G}$ satisfying

$$\lim_{n,m\to\infty} \Gamma(\xi_n,\xi_m) = \Gamma(\xi,\xi) = 0.$$

Every 0-Cauchy in $\mathcal{G}$ is a Cauchy, implying that all prtl. m. s.s are 0-complete. However, the opposite is not necessarily true.

Indeed, consider the set $\mathcal{G} = \mathbb{Q} \cap [0,\infty)$ endowed with the partial metric

$$\Gamma(\xi,\mathfrak{d}) = \max\{\xi,\mathfrak{d}\} \text{ for all } \xi,\mathfrak{d} \in \mathcal{G}.$$

Then it is a 0-complete that is not complete.

Let $\emptyset \neq \mathfrak{V}, \mathfrak{Y} \subseteq \mathfrak{G}$ where $(\mathfrak{G}, \Gamma)$ is a prtl. m. s.. Define the subsets

$$\mathfrak{V}_0 = \{\mathfrak{p} \in \mathfrak{V}: \Gamma(\mathfrak{p}, y) = \Gamma(\mathfrak{V}, \mathfrak{Y}) \text{ for some } y \in \mathfrak{Y}\},$$

and

$$\mathfrak{Y}_0 = \{y \in \mathfrak{Y}: \Gamma(\mathfrak{p}, y) = \Gamma(\mathfrak{V}, \mathfrak{Y}) \text{ for some } \mathfrak{p} \in \mathfrak{V}\},$$

where

$$\Gamma(\mathfrak{V}, \mathfrak{Y}) = \inf\{\Gamma(\mathfrak{p}, y): \mathfrak{p} \in \mathfrak{V},\ y \in \mathfrak{Y}\}.$$

Definition 3

A mapping $И: \mathfrak{V} \to \mathfrak{Y}$ is said to be a proximal contraction if there exists a constant $q \in [0,1)$ such that, for all $\xi_1, \xi_2, \mathfrak{p}_1, \mathfrak{p}_2 \in \mathfrak{V}$,

$$\Gamma(\xi_1, И\mathfrak{p}_1) = \Gamma(\mathfrak{V}, \mathfrak{Y}),$$
$$\Gamma(\xi_2, И\mathfrak{p}_2) = \Gamma(\mathfrak{V}, \mathfrak{Y})$$

implies

$$\Gamma(\xi_1, \xi_2) \leq q\,\Gamma(\mathfrak{p}_1, \mathfrak{p}_2)$$

where $(\mathfrak{G}, \Gamma)$ is a metric space

Definition 4

Let $\emptyset \neq \mathfrak{V}, \mathfrak{Y} \subseteq \mathfrak{G}$ where $(\mathfrak{G}, \Gamma)$ is a metric space. If every sequence $\{\mathfrak{p}_n\}$ in $\mathfrak{V}$ satisfying

$$\Gamma(\mathfrak{d}, \mathfrak{p}_n) \to \Gamma(\mathfrak{d}, \mathfrak{V}) \text{ for some } \mathfrak{d} \in \mathfrak{Y}$$

Has a convergent subsequence in $\mathfrak{G}$, we say that $\mathfrak{V}$ is said to be Γ-approximately compact w. r. to $\mathfrak{Y}$.

Proposition 1

Let $(\mathfrak{G}, \Gamma)$ be a complete metric space, $\emptyset \neq \mathfrak{V}, \mathfrak{Y} \subseteq \mathfrak{G}$ and $\mathfrak{V}_0 \neq \emptyset$. Assume that $\mathfrak{Y}$ is approximatively compact w. r. to $\mathfrak{V}$ and $\mathfrak{V}$ is closed. Then, $(\mathfrak{V}_0, \Gamma)$ is complete.

Now, we'll go over some key notions and notations from best proximity point theory in the context of prtl. m. s.s.

Definition 5

Let $\emptyset \neq \mathfrak{V}, \mathfrak{Y} \subseteq \mathfrak{G}$ where $(\mathfrak{G}, \Gamma)$ is a prtl. m. s. If every sequence $\{\mathfrak{p}_n\}$ in $\mathfrak{V}$ satisfying

$$\Gamma(\mathfrak{d}, \mathfrak{p}_n) \to \Gamma(\mathfrak{d}, \mathfrak{V}) \text{ for some } \mathfrak{d} \in \mathfrak{Y}$$

has a subsequence $\{\mathfrak{p}_{n_k}\}$ such that

$$\lim_{k,l\to\infty} \Gamma(\mathfrak{p}_{n_k}, \mathfrak{p}_{n_l}) = \lim_{k\to\infty} \Gamma(\mathfrak{p}_{n_k}, \mathfrak{p}) = \Gamma(\mathfrak{p}, \mathfrak{p}) = 0,$$

for some $\mathfrak{p} \in \mathfrak{V}$, then $\mathfrak{V}$ is said to be Γ-approximately compact w. r. to $\mathfrak{Y}$.

Theorem 1

Let $\emptyset \neq \mathfrak{V}, \mathfrak{Y} \subseteq \mathfrak{G}$ with $\mathfrak{V}_0 \neq \emptyset$ where $(\mathfrak{G}, \Gamma)$ is a complete metric space and $\mathfrak{Y}$ is approximatively compact with respect to $\mathfrak{V}$. Suppose $\mathfrak{V}$ is closed and $и: \mathfrak{V} \to \mathfrak{Y}$ is a continuous proximal contraction satisfying $И(\mathfrak{V}_0) \subseteq \mathfrak{Y}_0$. Then there is a unique point $\mathfrak{p} \in \mathfrak{V}$ satisfying

$$\Gamma(\mathfrak{p}, И\mathfrak{p}) = \Gamma(\mathfrak{V}, \mathfrak{Y}).$$

Definition 6

Let $(6, \Gamma)$ be a prtl. m. s. and let $И: 6 \to 6$ be a mapping. We say that И is continuous with respect to τ_Γ if

$$\lim_{r,m\to\infty} \Gamma(p_n, p_m) = \lim_{r\to\infty} \Gamma(p_n, p^*) = \Gamma(p^*, p^*),$$

then

$$\lim_{r,m\to\infty} \Gamma(Иp_n, Иp_m) = \lim_{r\to\infty} \Gamma(Иp_n, Иp^*) = \Gamma(Иp^*, Иp^*).$$

3-RESULTS

Firstly, we introduce the definition of a p-proximal Karapinar's contraction mapping.

Definition 7

Let $\emptyset \neq \mathfrak{V}, \mathfrak{Y} \subseteq 6$ where $(6, \Gamma)$ is a prtl. m. s.. A mapping $И: \mathfrak{V} \to \mathfrak{Y}$ is said to be a p-proximal Karapinar's contraction mapping if there exist real numbers $\aleph_1, \aleph_2, \aleph_3, \aleph_4, \aleph_5$ satisfying

i) $0 \leq \frac{\aleph_4 - \aleph_2}{\aleph_1 + \aleph_2} < 1$

ii) $\aleph_1 + \aleph_3 \neq 0$,

iii) $\aleph_1 + \aleph_2 + \aleph_3 > 0$,

iv) $\aleph_3 - \aleph_5 \geq 0$

such that

$$\begin{aligned} \Gamma(\zeta_1, Иp_1) &= \Gamma(\mathfrak{V}, \mathfrak{Y}), \\ \Gamma(\zeta_2, Иp_2) &= \Gamma(\mathfrak{V}, \mathfrak{Y}), \end{aligned}$$

imply

$$P(\aleph_1, \aleph_2, \aleph_3) \leq Q(\aleph_4, \aleph_5), \tag{1}$$

where

$$\begin{aligned} P(\aleph_1, \aleph_2, \aleph_3) &= \aleph_1 \Gamma(\zeta_1, \zeta_2) + \aleph_2[\Gamma(p_1, \zeta_1) + \Gamma(p_2, \zeta_2)] \\ &\quad + \aleph_3[\Gamma(p_2, \zeta_1) + \Gamma(p_1, \zeta_2)], \end{aligned}$$

and

$$Q(\aleph_4, \aleph_5) = \aleph_4 \Gamma(p_1, p_2) + \aleph_5(\Gamma(p_1, И\zeta_1) - \Gamma(\mathfrak{V}, \mathfrak{Y})),$$

for all $\zeta_1, \zeta_2, p_1, p_2 \in \mathfrak{V}$.

Theorem 2

Let $(6, \Gamma)$ be a complete prtl. m. s. and let $\emptyset \neq \mathfrak{V}, \mathfrak{Y} \subseteq 6$, where $\mathfrak{V}$ is closed and $\mathfrak{Y}$ is p-approximately compact w. r. to $\mathfrak{V}$, and $\mathfrak{V}_0 \neq \emptyset$. If $И: \mathfrak{V} \to \mathfrak{Y}$ is a p-proximal Karapinar's contraction mapping satisfying $И(\mathfrak{V}_0) \subseteq \mathfrak{Y}_0$ and the function $g(p) = \Gamma(p, Иp)$ is lower semicontinuous on $\mathfrak{V}$, then И has a best proximity point in $\mathfrak{V}$.

Proof

Let $p_0 \in \mathfrak{V}_0$ be arbitrary. Since $Иp_0 \in И(\mathfrak{V}_0) \subseteq \mathfrak{Y}_0$, there exists $p_1 \in \mathfrak{V}_0$ such that

$$\Gamma(p_1, Иp_0) = \Gamma(\mathfrak{V}, \mathfrak{Y}).$$

Similarly, there exists $p_2 \in \mathfrak{V}_0$ such that

$$\Gamma(\mathfrak{p}_2, И\mathfrak{p}_1) = \Gamma(\mathfrak{V}, \mathfrak{Y}). \tag{2}$$

Again, we can find a point $\mathfrak{p}_3 \in \mathfrak{V}_0$ such that

$$\Gamma(\mathfrak{p}_3, И\mathfrak{p}_2) = \Gamma(\mathfrak{V}, \mathfrak{Y}).$$

Repeating this process, we construct a sequence $\{\mathfrak{p}_n\}$ such that

$$\Gamma(\mathfrak{p}_{n+1}, И\mathfrak{p}_n) = \Gamma(\mathfrak{V}, \mathfrak{Y}),$$

for all $n \geq 1$. Since Иis a p-proximal Karapinar's contraction mapping, there exist constants $\mathfrak{r}_1, \mathfrak{r}_2, \mathfrak{r}_3, \mathfrak{r}_4, \mathfrak{r}_5$satisfying condition (1) such that

$$\begin{aligned} P(\mathfrak{r}_1, \mathfrak{r}_2, \mathfrak{r}_3) \quad &= \mathfrak{r}_1\Gamma(\mathfrak{p}_n, \mathfrak{p}_{n+1}) + \mathfrak{r}_2[\Gamma(\mathfrak{p}_{n-1}, \mathfrak{p}_n) + \Gamma(\mathfrak{p}_n, \mathfrak{p}_{n+1})] \\ &\quad + \mathfrak{r}_3[\Gamma(\mathfrak{p}_n, \mathfrak{p}_n) + \Gamma(\mathfrak{p}_{n-1}, \mathfrak{p}_{n+1})], \end{aligned} \tag{3}$$

and

$$Q(\mathfrak{r}_4, \mathfrak{r}_5) = \mathfrak{r}_4\Gamma(\mathfrak{p}_{n-1}, \mathfrak{p}_n) + \mathfrak{r}_5(\Gamma(\mathfrak{p}_{n-1}, И\mathfrak{p}_n) - \Gamma(\mathfrak{V}, \mathfrak{Y})), \tag{4}$$

for all $n \geq 1$. From eşitlikler (1), (2),(3) and (4), we obtain

$$(\mathfrak{r}_1 + \mathfrak{r}_2)\Gamma(\mathfrak{p}_n, \mathfrak{p}_{n+1}) + (\mathfrak{r}_3 - \mathfrak{r}_5)\Gamma(\mathfrak{p}_{n-1}, \mathfrak{p}_{n+1}) \leq (\mathfrak{r}_4 - \mathfrak{r}_2)\Gamma(\mathfrak{p}_{n-1}, \mathfrak{p}_n),$$

and hence

$$\Gamma(\mathfrak{p}_n, \mathfrak{p}_{n+1}) \leq k\,\Gamma(\mathfrak{p}_{n-1}, \mathfrak{p}_n),$$

where $k = \frac{\mathfrak{r}_4 - \mathfrak{r}_2}{\mathfrak{r}_1 + \mathfrak{r}_2} \in [0,1)$. By induction,

$$\begin{aligned} \Gamma(\mathfrak{p}_n, \mathfrak{p}_{n+1}) &\leq k\Gamma(\mathfrak{p}_{n-1}, \mathfrak{p}_n) \\ &\leq k^2\Gamma(\mathfrak{p}_{n-2}, \mathfrak{p}_{n-1}) \\ &\leq k^3\Gamma(\mathfrak{p}_{n-3}, \mathfrak{p}_{n-2}) \\ &\vdots \\ &\leq k^n\Gamma(\mathfrak{p}_0, \mathfrak{p}_1) \end{aligned}$$

for all $n \geq 1$. Moreover,

$$\begin{aligned} \Gamma(\mathfrak{p}_n, \mathfrak{p}_{n+p}) &\leq \sum_{i=0}^{p-1} \Gamma(\mathfrak{p}_{n+i}, \mathfrak{p}_{n+i+1}) - \sum_{i=1}^{p-1} \Gamma(\mathfrak{p}_{n+i}, \mathfrak{p}_{n+i}) \\ &\leq \sum_{i=0}^{p-1} k^{n+i}\,\Gamma(\mathfrak{p}_0, \mathfrak{p}_1) \\ &= \frac{1-k^p}{1-k} k^n \Gamma(\mathfrak{p}_0, \mathfrak{p}_1) \\ &\leq \frac{k^n}{1-k}\Gamma(\mathfrak{p}_0, \mathfrak{p}_1) \end{aligned}$$

Letting $n \to \infty$, we get

$$\lim_{n\to\infty} \Gamma(\mathfrak{p}_n, \mathfrak{p}_{n+p}) = 0,$$

so $\{p_n\}$ is a 0-Cauchy in $\mathfrak{V}$. Since $(6, \Gamma)$ is 0-complete and $\mathfrak{V}$ is closed, there exists $p^* \in \mathfrak{V}$ such that

$$\lim_{n\to\infty} \Gamma(p_n, p^*) = \lim_{m,n\to\infty} \Gamma(p_n, p_m) = \Gamma(p^*, p^*) = 0.$$

Using the partial metric inequality, we obtain

$$\lim_{n\to\infty} \Gamma(p^*, Ип_n) = \Gamma(p^*, \mathfrak{Y}).$$

Since $\mathfrak{Y}$ is p-approximately compact with respect to $\mathfrak{V}$, there exists a subsequence $\{Ип_{n_k}\}$ converging to some $y^* \in \mathfrak{Y}$ such that

$$\lim_{k\to\infty} \Gamma(Ип_{n_k}, y^*) = \lim_{k,l\to\infty} \Gamma(Ип_{n_k}, Ип_{n_l}) = \Gamma(y^*, y^*) = 0.$$

Consequently, we get

$$\Gamma(p^*, y^*) = \Gamma(\mathfrak{V}, \mathfrak{Y}).$$

Since $g(p) = \Gamma(p, Ип)$ is lower semicontinuous on $\mathfrak{V}$,

$$\begin{aligned} \Gamma(\mathfrak{V}, \mathfrak{Y}) &\le \Gamma(p^*, Ип^*) \\ &= g(p^*) \\ &\le \liminf g(p_{n_k}) \\ &= \Gamma(p^*, y^*) \\ &= \Gamma(\mathfrak{V}, \mathfrak{Y}) \end{aligned}$$

and hence

$$\Gamma(p^*, Ип^*) = \Gamma(\mathfrak{V}, \mathfrak{Y}).$$

Thus, $p^*$is a best proximity point of И. ■

Example 1

Let $6 = [0, \infty)$ and define

$$\Gamma(p, y) = \begin{cases} p, & p = y, \\ p + y, & p \neq y. \end{cases}$$

Then $(6, \Gamma)$ is a 0-complete prtl. m. s.. Take $\mathfrak{V} = [2,3]$, $\mathfrak{Y} = [0,1]$, and define

$$Ип = \begin{cases} 0, & p = 2, \\ 3 - p, & \text{otherwise.} \end{cases}$$

Indeed, let $\{p_n\}$ be a 0-Cauchy sequence in 6. Then we have

$$\lim_{n,m\to\infty} \Gamma(p_n, p_m) = 0 \Longrightarrow \lim_{n,m\to\infty} (p_n + p_m) = 0,$$

which implies

$$\lim_{n\to\infty} p_n = 0.$$

Hence, since every 0-Cauchy sequence in 6 converges to 0, $(6, \Gamma)$ is a 0-complete. Consider the subsets $\mathfrak{V} = [2,3]$ and $\mathfrak{Y} = [0,1]$. Since is a discrete metric space, $\mathfrak{V}$ is closed and $\mathfrak{V}$ is p-approximately compact w. r. to $\mathfrak{V}$. Also, it is clear that

$$\Gamma(\mathfrak{V},\mathfrak{Y}) = 2, \mathfrak{V}_0 = \{2\}, \mathfrak{Y}_0 = \{0\}.$$

Now, we define a mapping $И: \mathfrak{V} \to B$ by

$$Иp = \begin{cases} 0, & p = 2, \\ 3 - p, & \text{otherwise.} \end{cases}$$

Hence, we have $И(\mathfrak{V}_0) \subseteq B_0$. Next, we show that Иis a proximal Karapınar type nonunique contraction mapping. Let $\zeta_1, \zeta_2, p_1, p_2 \in \mathfrak{V}$ such that

$$\Gamma(\zeta_1, Иp_1) = \Gamma(\mathfrak{V}, V) \tag{5}$$

$$\Gamma(\zeta_2, Иp_2) = \Gamma(\mathfrak{V}, V) \tag{6}$$

The only points satisfying conditions (5) and (6) are

$$\zeta_1 = \zeta_2 = p_1 = p_2 = 2.$$

Hence, for all a_1, a_2, a_3, a_4, a_5satisfying conditions i-iv in Definition 7, we obtain

$$P(a_1, a_2, a_3) = 0 = Q(a_4, a_5),$$

and therefore Иis a p-proximal Karapınar type nonunique contraction mapping. Since $g(p) = \Gamma(p, Иp)$ is lower semicontinuous on $\mathfrak{V}$, all the hypotheses of Theorem 2 are satisfied. Hence, И has a best proximity point in $\mathfrak{V}$.

Theorem 3

Let $\emptyset \neq \mathfrak{V}, \mathfrak{Y} \subseteq \mathfrak{G}$, where $\mathfrak{V}$ is closed and $\mathfrak{V}_0 \neq \emptyset$ where $(\mathfrak{G}, \Gamma)$ is a complete prtl. m. s.. Suppose that $И(\mathfrak{V}_0) \subseteq \mathfrak{Y}_0$. И has a best proximity point in $\mathfrak{V}$ if $И: \mathfrak{V} \to \mathfrak{Y}$ is a continuous p-proximal Karapinar's contraction mapping.

Proof

As in the proof of Theorem 2, we can construct a subsequence $\{p_{n_k}\}$ of $\{p_n\}$ such that

$$\Gamma(p_{n_k+1}, Иp_{n_k}) = \Gamma(\mathfrak{V},\mathfrak{Y}).$$

Moreover,

$$\lim_{k\to\infty} \Gamma(p_{n_k+1}, p^*) = \lim_{k,l\to\infty} \Gamma(p_{n_k+1}, p_{n_l+1}) = \Gamma(p^*, p^*) = 0,$$

for some $p^* \in \mathfrak{V}$. Since И is continuous, we obtain

$$\lim_{k\to\infty} \Gamma(Иp_{n_k}, Иp^*) = \lim_{m,k\to\infty} \Gamma(Иp_{n_k}, Иp_m) = \Gamma(Иp^*, Иp^*) = 0.$$

Hence, we have

$$\Gamma(\mathfrak{V},\mathfrak{Y}) \leq \Gamma(p^*, Иp^*)$$

$$\leq \Gamma(p^*, p_{n_k+1}) + \Gamma(p_{n_k+1}, Иp_{n_k}) + \Gamma(Иp_{n_k}, Иp^*) - \Gamma(p_{n_k+1}, p_{n_k+1}) - \Gamma(Иp_{n_k}, Иp_{n_k}$$

$$\leq \Gamma(p^*, p_{n_k+1}) + \Gamma(p_{n_k+1}, Иp_{n_k}) + \Gamma(Иp_{n_k}, Иp^*)$$

$$\leq \Gamma(p^*, p_{n_k+1}) + \Gamma(\mathfrak{V},\mathfrak{Y}) + \Gamma(Иp_{n_k}, Иp^*)$$

Taking the limit as $k \to \infty$ in the last inequality, we obtain

$$\Gamma(p^*, Иp^*) = \Gamma(\mathfrak{V},\mathfrak{Y}).$$

Example 2

Let $\mathcal{G} = [0, \infty)$and $\Gamma: \mathcal{G} \times \mathcal{G} \to [0, \infty)$be a function defined by $\Gamma(\mathfrak{p}, y) = \max\{\mathfrak{p}, y\}$ for all $\mathfrak{p}, y \in \mathcal{G}$. Then, $(\mathcal{G}, \Gamma)$ is a prtl. m. s.. Also, it is 0-complete. Indeed, let $\{\mathfrak{p}_n\}$ be a 0-Cauchy in $\mathcal{G}$. Then, we have

$$\lim_{n,m\to\infty} \Gamma(\mathfrak{p}_n, \mathfrak{p}_m) = 0 \implies \lim_{n,m\to\infty} \max\{\mathfrak{p}_n, \mathfrak{p}_m\} = 0$$
$$\implies \lim_{n\to\infty} \mathfrak{p}_n = 0,$$

and so since every 0-Cauchy in $\mathcal{G}$ is only the sequence that converges to 0, $(\mathcal{G}, \Gamma)$ is a 0-complete prtl. m. s.. Consider the subset $\mathfrak{V} = [1,2]$ and $B = \left[0, \frac{1}{2}\right]$. Hence, $\mathfrak{V}$is closed and $\Gamma(\mathfrak{V}, \mathfrak{Y}) = 1$, $A_0 = \{1\}$and $B_0 = B$. Now, we define a mapping $И: \mathfrak{V} \to \mathfrak{Y}$ as

$$И\mathfrak{p} = 1 - \frac{\mathfrak{p}}{2}$$

Hence, we have that $И$is a continuous mapping satisfying $И(A_0) \subseteq B_0$. Now, we will show that $И$is a proximal Karapinar type nonunique contraction mapping. Let $\zeta_1, \zeta_2, \mathfrak{p}_1, \mathfrak{p}_2 \in \mathfrak{V}$ such that

$$\Gamma(\zeta_1, И\mathfrak{p}_1) = \Gamma(\mathfrak{V}, \mathfrak{Y}),$$
$$\Gamma(\zeta_2, И\mathfrak{p}_2) = \Gamma(\mathfrak{V}, \mathfrak{Y}).$$

The only points that satisfy this condition are $\zeta_1 = \zeta_2 = 1$for all $\mathfrak{p}_1, \mathfrak{p}_2 \in \mathfrak{V}$. Without loss of generality, let $\mathfrak{p}_2 \leq \mathfrak{p}_1$. We choose $\aleph_1 = 4$, $\aleph_2 = -1$, $\aleph_3 = \aleph_5 = 0$, $\aleph_4 = 3$. Hence, we have

i) $0 \leq \frac{\aleph_4 - \aleph_2}{\aleph_1 + \aleph_2} = \frac{3}{4} < 1$

ii) $\aleph_1 + \aleph_3 = 4 \neq 0$,

iii) $\aleph_1 + \aleph_2 + \aleph_3 = 3 > 0$,

iv) $\aleph_3 - \aleph_5 = 0 \geq 0$.

Also, we get

$$P(\aleph_1, \aleph_2, \aleph_3) = \aleph_1\Gamma(\zeta_1, \zeta_2) + \aleph_2(\Gamma(\mathfrak{p}_1, \zeta_1) + \Gamma(\mathfrak{p}_2, \zeta_2))$$
$$+\aleph_3(\Gamma(\mathfrak{p}_2, \zeta_1) + \Gamma(\mathfrak{p}_1, \zeta_2))$$
$$= 4 - \mathfrak{p}_1 - \mathfrak{p}_2,$$

And

$$Q(\aleph_4, \aleph_5) = \aleph_4\Gamma(\mathfrak{p}_1, \mathfrak{p}_2) + \aleph_5(\Gamma(\mathfrak{p}_1, И\zeta_1) - \Gamma(\mathfrak{V}, \mathfrak{Y}))$$
$$= 3\mathfrak{p}_1.$$

From the above expressions,

$$P(\aleph_1, \aleph_2, \aleph_3) \leq Q(\aleph_4, \aleph_5).$$

Hence, $И$ is a p-proximal Karapinar type nonunique contraction mapping. Since $g(\mathfrak{p}) = \Gamma(\mathfrak{p}, И\mathfrak{p})$ is lower semicontinuous on $\mathfrak{V}$, all hypotheses of Theorem 3 hold. Therefore, $И$ has a best proximity point in $\mathfrak{V}$.

By using the Proposition 1, we can present the following result

Theorem 4

Let $\emptyset \neq \mathfrak{B}, \mathfrak{Y} \subseteq \mathfrak{G}$, where $\mathfrak{B}$ is closed and $\mathfrak{B}_0 \neq \emptyset$ where $(\mathfrak{G}, \Gamma)$ is a prtl. m. s.. Suppose that $И(\mathfrak{B}_0) \subseteq \mathfrak{Y}_0$. И has a best proximity point in $\mathfrak{B}$ if $И: \mathfrak{B} \to \mathfrak{Y}$ is a continuous p-proximal Karapinar's contraction mapping and $(\mathfrak{B}_0, \mathfrak{G})$ is complete.

If we choose $\mathfrak{B}, \mathfrak{Y} \subseteq \mathfrak{G}$ such that $\mathfrak{G}(\mathfrak{B}, \mathfrak{Y}) = 0$, we can give the following result.

Corollary 1

Let $(\mathfrak{G}, \Gamma)$ be a complete prtl. m. s. and let $И: \mathfrak{G} \to \mathfrak{G}$ be continuous. If there exist real numbers $\mathfrak{r}_1, \mathfrak{r}_2, \mathfrak{r}_3, \mathfrak{r}_4, \mathfrak{r}_5$satisfying

i) $0 \leq \frac{\mathfrak{r}_4 - \mathfrak{r}_2}{\mathfrak{r}_1 + \mathfrak{r}_2} < 1$

ii) $\mathfrak{r}_1 + \mathfrak{r}_3 \neq 0$,

iii) $\mathfrak{r}_1 + \mathfrak{r}_2 + \mathfrak{r}_3 > 0$,

iv) $\mathfrak{r}_3 - \mathfrak{r}_5 \geq 0$

such that

$$\mathfrak{r}_1 \Gamma(И\mathfrak{p}_1, И\mathfrak{p}_2) + \mathfrak{r}_2[\Gamma(\mathfrak{p}_1, И\mathfrak{p}_1) + \Gamma(\mathfrak{p}_2, И\mathfrak{p}_2)]$$
$$+\mathfrak{r}_3[\Gamma(\mathfrak{p}_2, И\mathfrak{p}_1) + \Gamma(\mathfrak{p}_1, И\mathfrak{p}_2)] \leq \mathfrak{r}_4 \Gamma(\mathfrak{p}_1, \mathfrak{p}_2) + \mathfrak{r}_5 \Gamma(\mathfrak{p}_1, И^2\mathfrak{p}_1),$$

then И has a fixed point in $\mathfrak{G}$.

Since every metric space is prtl. m. s., we can give the following results.

Corollary 2

Let $(\mathfrak{G}, \Gamma)$ be a complete metric space and let $\emptyset \neq \mathfrak{B}, \mathfrak{Y} \subseteq \mathfrak{G}$, where $\mathfrak{B}$ is closed and $\mathfrak{Y}$ is approximately compact w. r. to $\mathfrak{B}$, and $\mathfrak{B}_0 \neq \emptyset$. If $И: \mathfrak{B} \to \mathfrak{Y}$ is a proximal Karapinar's contraction mapping satisfying $И(\mathfrak{B}_0) \subseteq \mathfrak{Y}_0$ and the function $g(\mathfrak{p}) = \Gamma(\mathfrak{p}, И\mathfrak{p})$ is lower semicontinuous on $\mathfrak{B}$, then И has a best proximity point in $\mathfrak{B}$.

Corollary 3

Let $(\mathfrak{G}, \Gamma)$ be a complete metric space and $И: \mathfrak{G} \to \mathfrak{G}$ be continuous. If there exist real numbers $\mathfrak{r}_1, \mathfrak{r}_2, \mathfrak{r}_3, \mathfrak{r}_4, \mathfrak{r}_5$satisfying

i) $0 \leq \frac{\mathfrak{r}_4 - \mathfrak{r}_2}{\mathfrak{r}_1 + \mathfrak{r}_2} < 1$

ii) $\mathfrak{r}_1 + \mathfrak{r}_3 \neq 0$,

iii) $\mathfrak{r}_1 + \mathfrak{r}_2 + \mathfrak{r}_3 > 0$,

iv) $\mathfrak{r}_3 - \mathfrak{r}_5 \geq 0$

such that

$$\mathfrak{r}_1 \Gamma(И\mathfrak{p}_1, И\mathfrak{p}_2) + \mathfrak{r}_2[\Gamma(\mathfrak{p}_1, И\mathfrak{p}_1) + \Gamma(\mathfrak{p}_2, И\mathfrak{p}_2)]$$
$$+\mathfrak{r}_3[\Gamma(\mathfrak{p}_2, И\mathfrak{p}_1) + \Gamma(\mathfrak{p}_1, И\mathfrak{p}_2)] \leq \mathfrak{r}_4 \Gamma(\mathfrak{p}_1, \mathfrak{p}_2) + \mathfrak{r}_5 \Gamma(\mathfrak{p}_1, И^2\mathfrak{p}_1),$$

then И has a fixed point in $\mathfrak{G}$

REFERENCES

[1] Aslanta¸s, M. (2024). Existence of the solution of nonlinear fractional differential equations via new best proximity point results. Mathematical Sciences, 18(4), 645-653.

[2] Banach, S.: Sur les opérations dans les ensembles abstraits et leur applications aux équations intégrales. Fund. Math, 3, 133.181 (1922).

[3] Basha, S. S.: Extensions of Banach.s contraction principle. Numer. Funct. Anal. Optim., 31 (5), 569-576 (2010).

[4] Basha, S. S., Veeramani, P.: Best approximations and best proximity pairs. Acta Sci. Math., 63, 289-300 (1977).

[5] Ciric, L.B , Samet, B., Aydi, H., Vetro, C.: Common fixed points of generalized contractions on partial metric spaces and an application. Applied Mathematics and Computation, 218(6), 2398-2406 (2011).

[6] Ciric, L.B, On some maps with a nonunique fixed point, Institute Mathe´matique, 17 (1974), 52-58.

[7] Du, W. S.: Some new results and generalizations in metric fixed point theory. Nonlinear Anal.,73 (5), 1439-1446 (2010).

[8] Gabeleh, M.: Best proximity points: global minimization of multivalued non-self mappings. Optimization Letters 8.3, 1101-1112 (2014).

[9] Gabeleh, M.: Global optimal solutions of non-self mappings. Sci. Bull..Politeh..Univ. Buchar., Ser. A, Appl. Math. Phys, 75, 67-74 (2013).

[10] Karapinar, E., Generalizations of Caristi Kirk.s theorem on partial metric spaces. Fixed Point Theory and Applications, 2011(1), 4 (2011).

[11] Karapinar, E. A New Non-Unique Fixed Point Theorem, J. Appl. Funct. Anal. , 7(2012),no:1-2,92-97.

[12] E. Karapınar and S. Romaguera, Nonunique .xed point theorems in partial metric spaces, Filomat, 27(7), (2013), 1305-1314.

[13] Matthews, S.G.: Partial metric topology. Ann. New York Acad. Sci., 728, 183-197 (1994)

[14] Nastasi, A., Vetro, P., Radenovi´c, S.: Some .xed point results via R-functions. Fixed Point Theory and Applications, 2016(1), 1-12 (2016).

[15] B.G. Pachpatte, On C´ iric´ type maps with a non-unique fixed point, Indian J. Pure Appl. Math., 10 (1979), 1039.1043.

[16] Reich, S.: Some problems and results in .xed point theory. Contemp. Math, 21, 179-187 (1983).

[17] Reich, S.: Fixed points of contractive functions. Boll. Unione Mat. Ital.,5, 26-42 (1972).

[18] Romaguera, S.: A Kirk type characterization of completeness for partial metric spaces. Fixed Point Theory and Applications, 2009,1: 493298 (2010).

[19] Romaguera, S.: On Nadler.s fixed point theorem for partial metric spaces. Mathematical Sciences and Applications E-Notes, 1(1), 1-8 (2013)

Chapter 6

OPTIMAL CONTROL PROBLEMS FOR THE SCHRÖDINGER EQUATION: THEORY, METHODS, AND APPLICATIONS

Bünyamin Yıldız[1]

1 Department of Mathematics, Faculty of Arts and Sciences

Hatay Mustafa Kemal University, Hatay, Turkey

ORCID-ID: 0000-0002-0792-9520

1. Introduction

Optimal control of partial differential equations is a highly active and rapidly developing field within applied mathematics, with significant applications in physics, engineering, economics, and many other scientific disciplines. Among these, optimal control problems governed by the Schrödinger equation hold particular importance due to their fundamental role in quantum mechanics and quantum technologies.

The temporal evolution of quantum states is dictated by the Schrödinger equation, a cornerstone of physics established by Erwin Schrödinger in 1926. By governing the dynamics of the wave function, this equation encodes all probabilistic data regarding a system's observable properties. In contemporary research, applying optimal control theory to these quantum systems has become a priority, driven by applications in quantum information processing, computing, and the precise manipulation of chemical reactions using lasers.

The class of optimal control problems considered here for the nonstationary Schrödinger equation of quasi-optics deal with the dispersion of light beams in inhomogeneous propagation media. In these types of problems, the refractive coefficient or absorption coefficient is usually considered as the control of the system. Such problems arise naturally in adaptive optics, where one seeks to optimize the shape of optical elements to minimize aberrations caused by atmospheric turbulence or other disturbances.

A primary obstacle in quantum mechanics is the reconstruction of the potential function, commonly known as the inverse problem. Since this task is ill-posed according to Hadamard's criteria, it imposes significant difficulties on both theoretical analysis and numerical computation. Consequently, this complexity has driven advancements in scattering theory, where interaction potentials are identified by using energy minimization techniques to fit empirical scattering data.This chapter presents a systematic study of optimal control problems for Schrödinger equations, covering both linear and nonstationary cases. We investigate the well-posedness of the optimal control problem, focusing on unique existence of solutions, derive necessary and sufficient optimality conditions, and establish the differentiability of cost functionals. Our approach integrates tools from functional analysis, the theory of partial differential equations, and optimal control.

2. Mathematical Preliminaries

2.1. Function Spaces and Norms

Let $C^0([0,T], B)$ denote the Banach space of all functions with values in a Banach space B which are continuous on the interval [0,T]. In this space, the norm is defined as:

$$\|u(t)\|_{C^0([0,T],B)} = \max_{0\le t\le T} \|u(t)\|_B$$

For the spatial and temporal domains, we consider $x \in [0,l]$, $t \in [0,T]$, and $z \in [0,L]$, where l, T, and L are positive real numbers. We define the following domains:

- $\Omega = (0,l) \times (0,T) \times (0,L)$ — the full space-time domain
- $\Omega_L = (0,l) \times (0,L)$ — the spatial domain at fixed time
- $\Omega_T = (0,l) \times (0,T)$ — the space-time domain at fixed z
- $S = (0,T) \times (0,L)$ — the boundary surface

The space $L^2(\Omega)$ is the well-known Lebesgue space consisting of all functions defined in Ω that are measurable and square-integrable. For $k, m \ge 0$, the Sobolev space $W_2^{k,m}(\Omega)$ is defined as in Ladyzhenskaya's classical treatise on boundary value problems of mathematical physics.

2.2. Hilbert Space Structure for Complex Functions

The space $W_2^{2,1,1}(\Omega)$ is a Hilbert space under the inner product:

$$\langle \psi, \varphi \rangle_{W_2^{2,1,1}(\Omega)} = \iiint_\Omega [\psi\bar{\varphi} + (\partial\psi/\partial x)(\partial\bar{\varphi}/\partial x) + (\partial^2\psi/\partial x^2)(\partial^2\bar{\varphi}/\partial x^2) + (\partial\psi/\partial t)(\partial\bar{\varphi}/\partial t) + (\partial\psi/\partial z)(\partial\bar{\varphi}/\partial z)] \, dx\, dt\, dz$$

where $\bar{\varphi}$ denotes the complex conjugate of φ. Induced by this inner product we have the following norm:

$$\|\psi\|_{W_2^{2,1,1}(\Omega)} = \sqrt{\langle \psi, \psi \rangle_{W_2^{2,1,1}(\Omega)}}$$

This Hilbert space structure is essential for the variational formulation of optimal control problems and for establishing the existence of optimal controls through weak compactness arguments.

3. Optimal Control Problem for the Nonstationary Schrödinger Equation

3.1. Problem Formulation

Let us consider the optimal control problem for minimizing the cost functional:

$$J_\alpha(v) = \beta_0 \iint_{\Omega_L} |\psi(x,T,z) - y_0(x,z)|^2 \, dx\, dz + \beta_1 \iint_{\Omega_T} |\psi(x,t,L) - y_1(x,t)|^2 \, dx\, dt + \alpha\|v - \omega\|^2_H$$

on the admissible set V defined by:

$$V = \{v = (v_0, v_1) : v_0 \in L^2(\Omega_L), v_1 \in L^2(\Omega_T), \|v_0\|_{L^2(\Omega_L)} \le b_0, \|v_1\|_{L^2(\Omega_T)} \le b_1\}$$

The state equation is the nonstationary Schrödinger equation of quasi-optics:

$$i(\partial\psi/\partial t) + ia_0(\partial\psi/\partial z) - a_1(\partial^2\psi/\partial x^2) + a_2(x)\psi + ia(x,t,z)\psi = f(x,t,z), \; (x,t,z) \in \Omega$$

subject to the initial conditions:

$$\psi(x,0,z) = v_0(x,z), \; (x,z) \in \Omega_L$$
$$\psi(x,t,0) = v_1(x,t), \; (x,t) \in \Omega_T$$

and the Neumann boundary conditions:

$$(\partial\psi/\partial x)(0,t,z) = (\partial\psi/\partial x)(l,t,z) = 0, \; (t,z) \in S$$

Here, $i^2 = -1$ is the imaginary unit, $a_0 > 0$, $a_1 > 0$ are positive constants, and the coefficient functions $a_2(x)$ and $a(x,t,z)$ are bounded measurable functions satisfying:

$$\mu_0 \le a_2(x) \le \mu_1, \; \forall x \in (0,l)$$
$$0 \le a(x,t,z) \le \mu_2, \; \forall (x,t,z) \in \Omega$$

where $\mu_j > 0$ ($j = 0,1,2$) are positive constants. The parameters $\beta_0 \ge 0$, $\beta_1 \ge 0$ with $\beta_0 + \beta_1 \ne 0$ are weighting coefficients in the cost functional, and $\alpha \ge 0$ is a regularization parameter.

3.2. Generalized Solution Concept

For each control $v \in V$, we seek a generalized solution $\psi = \psi(x,t,z;v)$ belonging to the space:

$$B_0 = C^0([0,T], L^2(\Omega_L)) \cap C^0([0,L], L^2(\Omega_T))$$

The generalized solution satisfies an integral identity involving test functions $\eta \in W_2^{2,1,1}(\Omega)$ with $(\partial\eta/\partial x)(0,t,z) = (\partial\eta/\partial x)(l,t,z) = 0$. Using standard results from the boundary value problem theory in mathematical physics together with the Galerkin approach, one can establish that for every $v \in V$, the solution of the boundary value problem exists in B_0, is unique, and this solution indeed satisfies the a priori estimate:

$$\|\psi(\cdot,t,\cdot)\|_{L^2(\Omega\_L)} + \|\psi(\cdot,\cdot,z)\|_{L^2(\Omega\_T)} \le c_0(\|v_0\|_{L^2(\Omega\_L)} + \|v_1\|_{L^2(\Omega\_T)} + \|f\|_{L^2(\Omega)})$$

where c_0 is a constant that is independent of the data. This estimate is fundamental for establishing the continuity of the solution map and, consequently, the continuity of the cost functional.

3.3. Existence and Uniqueness of Optimal Control

The following theorem establishes the fundamental well-posedness result for the optimal control problem.

Theorem 3.1. *Suppose that $\alpha \ge 0$ and the functions $a_2(x)$, $a(x,t,z)$, $y_0(x,z)$, $y_1(x,t)$, $f(x,t,z)$ satisfy the stated conditions. Then the optimal control problem must have at least one solution. If $\alpha > 0$, then the solution is unique, and for this solution the following stability estimate holds:*

$$\|v_m - v^*\|^2\_H \le c_1(J\_\alpha(v_m) - J^*\_\alpha),\ m = 1, 2, \ldots$$

where $v^* \in V$ is the optimal control, $\{v_m\} \subset V$ is a minimizing sequence, $J^*\_\alpha = \inf\_{v\in V} J\_\alpha(v)$, and c_1 is a constant which is independent of m.

Proof Outline. The proof proceeds in several steps:

Step 1 (Continuity): We first show that $J\_\alpha(v)$ is continuous on V for $\alpha \ge 0$. Taking an arbitrary $v \in V$ and its increment $\Delta v \in H$, the increment of the state function $\Delta\psi$ satisfies a homogeneous boundary value problem of the same type. Using the a priori estimates, we obtain $|\Delta J\_\alpha(v)| \le c_4(\|\Delta v\|\_H + \|\Delta v\|^2\_H)$, which implies continuity.

Step 2 (Convexity): We establish that $J\_\alpha(v)$ is convex on V. Using the linearity of the state equation, we show that $\psi(x,t,z;\ \beta v + (1-\beta)w) = \beta\psi(x,t,z;v) + (1-\beta)\psi(x,t,z;w)$ for all $v, w \in V$ and $\beta \in [0,1]$. This leads to the inequality $J\_\alpha(\beta v + (1-\beta)w) \le \beta J\_\alpha(v) + (1-\beta)J\_\alpha(w) - \alpha\beta(1-\beta)\|v-w\|^2\_H$.

Step 3 (Weak Semicontinuity): Since $J\_\alpha(v)$ is continuous and convex on V, it is weakly lower semicontinuous on V.

Step 4 (Existence): The set V is weakly compact in the Hilbert space $H = L^2(\Omega\_L) \times L^2(\Omega\_T)$. Therefore, $J\_\alpha(v)$ attains its minimum on V.

Step 5 (Uniqueness for $\alpha > 0$): When $\alpha > 0$, the functional $J\_\alpha(v)$ is strongly convex, which implies strict convexity and hence uniqueness of the minimum point. □

3.4. Differentiability of the Cost Functional

To derive necessary optimality conditions, we need to establish the Fréchet differentiability of the cost functional. This requires introducing the adjoint problem.

The Adjoint Problem. Let $\varphi = \varphi(x,t,z)$ be the solution of the conjugate (adjoint) problem:

$$i(\partial\varphi/\partial t) + ia_0(\partial\varphi/\partial z) - a_1(\partial^2\varphi/\partial x^2) + a_2(x)\varphi - ia(x,t,z)\varphi = 0,\ (x,t,z) \in \Omega$$
$$\varphi(x,T,z) = -2i\beta_0(\psi(x,T,z) - y_0(x,z)),\ (x,z) \in \Omega\_L$$
$$\varphi(x,t,L) = -(2i\beta_1/a_0)(\psi(x,t,L) - y_1(x,t)),\ (x,t) \in \Omega\_T$$
$$(\partial\varphi/\partial x)(0,t,z) = (\partial\varphi/\partial x)(l,t,z) = 0,\ (t,z) \in S$$

This adjoint problem is a backward-in-time boundary value problem for the Schrödinger equation. Through the variable transformation $\tau = T - t$, $\theta = L - z$, one can show that this problem is indeed equivalent to a forward problem of the same type, ensuring unique existence of the solution $\varphi \in B_0$.

Theorem 3.2. *The functional $J_\alpha(v)$ is Fréchet differentiable on V, and the gradient is given by:*

$$J'_\alpha(v) = (J'_{\alpha 01}(v), J'_{\alpha 02}(v), J'_{\alpha 11}(v), J'_{\alpha 12}(v))$$

where the components are:

- $J'_{\alpha 01}(v) = \mathrm{Re}(\varphi(x,0,z)) + 2\alpha\, \mathrm{Im}(v_0(x,z) - \omega_0(x,z))$
- $J'_{\alpha 02}(v) = -\mathrm{Im}(\varphi(x,0,z)) + 2\alpha\, \mathrm{Re}(v_0(x,z) - \omega_0(x,z))$
- $J'_{\alpha 11}(v) = \mathrm{Re}(\varphi(x,t,0)) + 2\alpha\, \mathrm{Im}(v_1(x,t) - \omega_1(x,t))$
- $J'_{\alpha 12}(v) = -\mathrm{Im}(\varphi(x,t,0)) + 2\alpha\, \mathrm{Re}(v_1(x,t) - \omega_1(x,t))$

3.5. Necessary and Sufficient Optimality Conditions

Theorem 3.3. *Suppose that the assertions of Theorem 3.2 hold. The necessary and sufficient condition for $v^* \in V$ to be the solution of the optimal control problem is:*

$$\langle J'_\alpha(v^*), v - v^* \rangle_H \geq 0, \ \forall v \in V$$

This variational inequality characterizes the optimal control as the projection of the unconstrained minimizer onto the admissible set V. The condition is both necessary (from convexity) and sufficient (from the strict convexity when $\alpha > 0$).

4. Optimization of Systems Described by the Linear Schrödinger Equation

4.1. Problem Statement and Estimates

We turn our attention to control problems governed by the linear Schrödinger equation. The core objective here is to identify a control strategy that minimizes a defined performance index. This minimization must occur while satisfying the constraints imposed by the linear Schrödinger equation, along with the requisite boundary and initial data..

Let the spatial domain be $\Omega = (0, l)$ and the time interval be $(0, T)$. We consider the linear Schrödinger equation:

$$i(\partial\psi/\partial t) + (\partial^2\psi/\partial x^2) - q(x)\psi = 0, \ (x,t) \in \Omega \times (0,T)$$

with initial condition $\psi(x,0) = \psi_0(x)$ and homogeneous Dirichlet boundary conditions $\psi(0,t) = \psi(l,t) = 0$. Here, $q(x)$ represents the potential in quantum mechanics, which is the quantity to be determined or controlled.

With the aim of addressing this optimal control problem, two fundamental estimates have been established. These estimates provide stability bounds for the solution and are essential for proving existence and deriving optimality conditions.

4.2. First Estimate

Theorem 4.1. *Let ψ be the solution of the linear Schrödinger equation with potential q. Then the following estimate holds:*

$$\|\psi(\cdot,t)\|^2_{L^2(\Omega)} \leq C_1 \exp(C_2 t)\, \|\psi_0\|^2_{L^2(\Omega)}$$

where C_1 and C_2 are positive constants depending on the potential q and the domain Ω.

This estimate shows that the L^2 norm of the solution at any time t is controlled by the initial data, with at most exponential growth in time. The constants C_1 and C_2 can be explicitly computed in terms of bounds on the potential.

4.3. Second Estimate

Theorem 4.2. *Under the same conditions, the gradient of the solution satisfies:*

$$\|\partial\psi/\partial x(\cdot,t)\|^2_{L^2(\Omega)} \leq C_3 \exp(C_4 t) \left(\|\psi_0\|^2_{H^1(\Omega)} + \|q\|^2_{L^\infty(\Omega)} \|\psi_0\|^2_{L^2(\Omega)}\right)$$

This second estimate provides control over the spatial gradient of the solution, which is important for establishing regularity and for the analysis of inverse problems involving the determination of the potential from boundary measurements.

4.4. Conditions for Optimality in the Linear Framework

When addressing the linear Schrödinger equation, the optimization problem can be constructed using various objective functions, such as those based on terminal states, boundary observations, or Lions-type functionals. In each case, optimality is characterized by conditions derived using variational techniques together with Lagrange multiplier methods. While general control theory guarantees the unique existence of solutions, the explicit structure of the optimality conditions varies according to the selected cost functional and the set of admissible controls. Crucially, the adjoint system is utilized to compute the gradient of the cost functional and to characterize the optimal control through a variational inequality.

5.1. Quantum Optimal Control Theory

Quantum optimal control has evolved into one of the cornerstones for enabling quantum technologies. The field has seen rapid evolution and expansion in recent years, with applications ranging from quantum computing and quantum information processing to laser control of chemical reactions and adaptive optics.

The primary objective of quantum control theory is the development of methods capable of manipulating and controlling quantum systems. The advent of laser femtosecond pulses marked a significant shift in the field, with subsequent research concentrating on optimizing laser pulse shapes as a key control strategy. This involves iterative modifications to the laser pulse shape, optimizing the result of a predetermined reaction product until the desired outcome is realized.

Modern quantum optimal control encompasses several key areas:

1. Initial state preparation and gate implementation in quantum computing
2. Laser control of molecular dynamics and chemical reactions
3. Adaptive optics for astronomical observations and laser beam propagation
4. Nuclear magnetic resonance (NMR) pulse sequence optimization
5. Quantum error correction and decoherence control

5.2. Controllability and Observability

Recent advances have established important controllability results for the Schrödinger equation. The exact controllability in $H^{-1}(\Omega)$ with L^2-boundary control has been proved, as well as the exact controllability in $L^2(\Omega)$ with L^2-controls supported in a neighborhood of the boundary. Both results hold for arbitrarily small time, demonstrating the strong controllability properties of the Schrödinger equation.

The method of proof combines the, introduced by J.-L. Lions, Hilbert Uniqueness Method (HUM) with multiplier techniques. These controllability results have important implications for inverse problems, as they establish the observability of the system from boundary measurements.

5.3. Inverse Problems and Parameter Identification

A significant application of optimal control theory for Schrödinger equations is in solving inverse problems. These include:

Potential Determination: The reconstruction of quantum potentials from boundary or spectral information constitutes an inverse problem, for which variational strategies grounded in optimal control are employed to stabilize the solution.

Coefficient Identification: Determining spatially varying coefficients in the Schrödinger equation from partial boundary measurements. Carleman estimates have been used to establish uniqueness and stability results for such problems.

Source Identification: The boundary control method has been successfully applied to solve dynamical inverse problems for the Schrödinger equation, recovering spectral data from dynamical boundary observations.

5.4. Neural Network and Machine Learning Implementations

Contemporary studies have investigated the use of neural networks to address optimal control challenges within the Schrödinger framework. These methods typically employ a hybrid strategy, merging sampling-driven training protocols with efficient time-splitting spectral algorithms, particularly for systems in the semiclassical regime. Deep learning techniques have proven especially robust for problems involving uncertain or randomized potentials. Numerical experiments confirm that these neural network architectures deliver high accuracy and computational efficiency when handling stochastic control problems.

5.5. Phase-Space Formulations and Wigner Equation

The Wigner quasi-density function provides a phase-space formulation of statistical quantum mechanics that is of fundamental importance in theoretical investigation and applications. Recent work has contributed to the formulation and analysis of optimal control problems for the Wigner equation, which describes the time evolution of the quasi-density function.

For such problems, two possible control mechanisms have been considered: control through the potential and control through the initial state. A detailed analysis in weighted Sobolev spaces for the controlled nonhomogeneous Wigner equation has been developed, along with theoretical results concerning existence of optimal controls, differentiability of the control-to-state map, and the derivation of optimality systems.

6. Numerical Methods and Computational Aspects

6.1. Gradient-Based Optimization Methods

A range of computational techniques have been given to address optimal control problems involving the Schrödinger equation. Among these, the predominant strategy is gradient-based optimization. In this framework, the gradient of the objective function is typically calculated via the adjoint state formalism, as detailed in Section 3.4.

The basic algorithm proceeds as follows:

Step 1. Choose an initial guess v^0 for the control.
Step 2. Solve the state equation forward in time to obtain $\psi(x,t,z;v^n)$.
Step 3. Solve the adjoint equation backward in time to obtain $\varphi(x,t,z;v^n)$.
Step 4. Compute the gradient $J'_\alpha(v^n)$ using the formulas in Theorem 3.2.
Step 5. Update the control: $v^{n+1} = P_V(v^n - \tau_n J'_\alpha(v^n))$, where P_V is the projection onto V and τ_n is a step size.
Step 6. Repeat until convergence.

6.2. Krotov Iteration Method

The Krotov method is a powerful iterative technique specifically designed for quantum optimal control problems. Unlike gradient descent methods, the Krotov method uses a different update formula that can provide faster convergence, particularly for problems with complex control landscapes.

The method can be explained as constructing an auxiliary functional that bounds the original cost functional from below and is maximized at each iteration. This approach ensures monotonic convergence and can avoid local minima that plague gradient-based methods.

6.3. Spectral Methods and Artificial Boundary Conditions

Spectral techniques offer a robust framework for addressing quantum optimal control challenges, especially when implemented alongside artificial boundary conditions. The fundamental strategy involves leveraging the Laplace transform and its inverse to shift the problem into the frequency domain, thereby effectively managing computational complexity.

For problems with periodic potentials, the resulting formulations are well-suited for direct numerical treatment using conventional methods for bounded domains. The artificial boundary conditions allow truncation of unbounded domains while maintaining accuracy through transparent or absorbing boundary conditions.

7. Physical and Engineering Applications

We focus in the practical implications of the optimal control theory developed for the Schrödinger equation in this section. While the theoretical framework ensures rigor, its utility is best demonstrated through specific applications in optical engineering, quantum information science, and physical chemistry.

7.1. Quasi-Optics and Beam Dynamics

In the study of quasi-optics, the behavior of paraxial light beams traveling through nonlinear and inhomogeneous media is described by the nonstationary Schrödinger equation (known in fiber optics as the NLSE). A defining feature of this framework is the mathematical parallel it draws: the spatial progression of the beam along its propagation axis is treated as the evolutionary variable, equivalent to time in traditional quantum mechanics.

Minimization of Aberrations: The optimal control framework provides a robust mathematical basis for designing optical elements (such as graded-index fibers or diffractive lenses) that minimize phase distortions. By defining a cost functional that penalizes deviations from a target intensity profile, one can solve for the optimal refractive index distribution.

Adaptive Optics: In astronomical applications, atmospheric turbulence introduces stochastic phase errors. Optimal control algorithms are employed in real-time to adjust the shape of deformable mirrors, thereby compensating for wavefront distortions and restoring high-resolution imaging capabilities.

Telecommunications: In optical fiber communications, signal integrity is compromised by chromatic dispersion and nonlinearity. Optimal control theory can be used to design soliton management systems and pulse-shaping techniques that maintain pulse coherence over long distances, maximizing bandwidth and minimizing bit-error rates.

7.2. Quantum Computing and Information Processing

Quantum optimal control (QOC) has transitioned from a theoretical curiosity to a cornerstone of modern quantum technology. As quantum hardware scales up, the precise manipulation of qubit dynamics becomes increasingly challenging due to environmental noise and system imperfections.

Pulse Sequence Design: The central problem involves finding control fields (e.g., microwave or laser pulses) that drive the system unitary evolution operator to a target quantum gate. Techniques such as GRAPE (Gradient Ascent Pulse Engineering) and Krotov's method utilize the adjoint state formulation derived in previous chapters to iteratively optimize these control fields.

High-Fidelity Gates: Implementing universal gates like CNOT or Hadamard with fidelities exceeding the fault-tolerance threshold is critical. QOC allows for the suppression of leakage into non-computational subspaces and the mitigation of crosstalk between adjacent qubits.

Quantum Error Correction: Beyond passive stabilization, active control is used to implement dynamic decoupling sequences that average out environmental noise, effectively extending the coherence time of the quantum states.

Adiabatic Quantum Computing: For annealing-based approaches, optimal control determines the optimal annealing schedule—the rate at which the Hamiltonian changes—to ensure the system remains in its ground state, preventing diabatic transitions that lead to computational errors.

7.3. Laser Control of Chemical Reactions

Coherent control of molecular dynamics represents a fusion of quantum mechanics and femtosecond laser technology. The objective is to steer the quantum wave packet of a molecule on its potential energy surface towards a desired product channel.

Selective Bond Breaking: Traditional chemistry relies on thermal activation, which is statistical and often non-selective. In contrast, optimal laser control can deposit energy into a specific vibrational mode, facilitating the breaking of a strong bond while leaving weaker bonds intact.

Interference of Quantum Pathways: Methods such as the Brumer-Shapiro approach or stimulated Raman adiabatic passage (STIRAP) rely on the constructive or destructive interference of different reaction pathways. The optimal control framework systematically identifies the precise amplitude and phase modulation of the laser pulse required to maximize the yield of the target isomer or dissociation product.

High-Harmonic Generation: Beyond standard reactions, these techniques are also applied to optimize the generation of high-order harmonics, paving the way for attosecond physics and electron dynamics control.

8. Conclusions and Future Directions

This work has provided an in-depth examination of control problems subject to the Schrödinger constraint. Our approach successfully merges abstract mathematical foundations with practical numerical algorithms, resulting in a unified framework capable of addressing key challenges in quantum control. The main contributions of this work are outlined below.

Well-posedness Analysis: We established the existence and uniqueness of optimal controls for both linear and nonstationary Schrödinger equations. By employing semigroup theory and a priori estimates, we ensured that the control problems are mathematically meaningful under appropriate regularity conditions on the initial data and potentials.

Sensitivity Analysis: We derived the Fréchet differentiability of various cost functionals. Using the adjoint problem technique, we provided explicit, computationally efficient gradient formulas, which are prerequisite for any first-order optimization algorithm.

Optimality Conditions: We established necessary and sufficient optimality conditions expressed as variational inequalities. These conditions not only characterize the optimal solutions but also serve as the foundation for verifying numerical convergence.

Survey of Advanced Topics: We reviewed significant recent developments, including exact controllability results, the solution of inverse problems (identifying potentials from boundary measurements), and the emerging intersection with data-driven approaches.

Numerical and Practical Integration: We discussed the discretization of these infinite-dimensional problems and demonstrated their relevance in cutting-edge applications across quantum technologies, nonlinear optics, and femtochemistry.

Future Directions:

Although significant progress has been made, several open problems and avenues for future research remain:

Open Quantum Systems: A critical avenue for future research involves generalizing the proposed framework to accommodate master equations, such as the Lindblad formalism. This expansion is indispensable for accurately capturing decoherence and dissipative phenomena, which are unavoidable in larger, realistic quantum systems.

Machine Learning Integration: To address the substantial computational burden associated with traditional iterative solvers, recent research points toward coupling Deep Reinforcement Learning (DRL) with classical optimal control. This hybrid approach presents a highly effective strategy for achieving faster, more efficient solutions. Neural networks could potentially approximate the mapping from target states to optimal control pulses.

In the context of quantum sensing, the application of the control strategies developed in this work has the potential to substantially improve the sensitivity and precision of quantum metrology devices, including but not limited to gravimeters and atomic clocks, thereby providing a clear route toward both technological innovation and practical scientific applications.

The theoretical framework developed in this chapter offers a solid and systematic foundation for addressing the challenges inherent in controlling quantum systems. By establishing rigorous analytical tools and control mechanisms, this framework significantly broadens our ability to steer and optimize quantum dynamics, ultimately facilitating the transition of these technologies from theoretical models to experimentally realizable and commercially viable systems.

References

[1] Yıldız, B., Kılıçoğlu, O., & Yagubov, G. (2009). Optimal control problem for nonstationary Schrödinger equation. *Numerical Methods for Partial Differential Equations, 25*, 1195-1203.

[2] Yıldız, B., & Subaşı, M. (2001). On the optimal control problem for linear Schrödinger equation. *Applied Mathematics and Computation, 121*, 373-381.

[3] Yıldız, B., & Yagubov, G. (1997). On an optimal control problem. *Journal of Computational and Applied Mathematics, 88*, 275-287.

[4] Iskenderov, A.D., & Yagubov, G.Ya. (1989). Optimal control of non-linear quantum-mechanical systems. *Automation and Remote Control, 50*, 1631-1641.

[5] Lions, J.-L. (1971). *Optimal Control of Systems Governed by Partial Differential Equations*. Springer-Verlag, Berlin.

[6] Ladyzhenskaya, O.A. (1986). *Boundary Value Problems of Mathematical Physics*. American Mathematical Society.

[7] Vasilev, F.P. (1981). *Numerical Methods for Solving Extremal Problems*. Nauka, Moscow.

[8] Machtyngier, E. (1994). Exact controllability for the Schrödinger equation. *SIAM Journal on Control and Optimization, 32*, 24-34.

[9] Koch, C.P., et al. (2022). Quantum optimal control in quantum technologies. Strategic report. *EPJ Quantum Technology, 9*, Article 19.

[10] Morandi, O., Rotundo, N., Borzì, A., & Barletti, L. (2024). An optimal control problem for the Wigner equation. *SIAM Journal on Applied Mathematics, 84*, 387-413.

[11] Aronna, M.S., Bonnans, J.F., & Kröner, A. (2019). Optimal control of PDEs in a complex space setting. *SIAM Journal on Control and Optimization, 57*, 1390-1416.

[12] Li, S., et al. (2023). On a neural network approach for solving potential control problem of the semiclassical Schrödinger equation. *Journal of Computational Physics, 495*, 112562.

[13] Yagubov, G.Ya., & Musayeva, M.A. (1997). On the identification problem for nonlinear Schrödinger equation. *Differential Equations, 33*, 1691-1698.

[14] Avdonin, S., & Belishev, M.I. (2002). Solving the dynamical inverse problem for the Schrödinger equation by the boundary control method. *Inverse Problems, 18*, 349-361.

[15] Baudouin, L., & Puel, J.-P. (2002). Uniqueness and stability in an inverse problem for the Schrödinger equation. *Inverse Problems, 18*, 1537-1554.

[16] Vorontsov, M.A., & Shmalgauzen, V.I. (1985). *The Principles of Adaptive Optics*. Nauka, Moscow.

[17] Lebeau, G. (1992). Contrôle de l'équation de Schrödinger. *Journal de Mathématiques Pures et Appliquées, 71*, 267-291.

[18] Khaneja, N., et al. (2005). Optimal control of coupled spin dynamics. *Journal of Magnetic Resonance, 172*, 296-305.

[19] Brif, C., Chakrabarti, R., & Rabitz, H. (2010). Control of quantum phenomena. *Advances in Chemical Physics, 148*, 1-76.

[20] D'Alessandro, D. (2007). *Introduction to Quantum Control and Dynamics*. Chapman & Hall/CRC.